ChemPubSoc Europe

DOI: 10.1002/ejic.201600394

EurJIC European Journal of Inorganic Chemistry

Microreview

CLUSTER ISSUE

Postsynthetic Modification

Postsynthetic Modification of Zirconium Metal-Organic Frameworks

Ross J. Marshall[a] and Ross S. Forgan*[a]

Abstract: Metal-organic frameworks (MOFs) have been in the spotlight for a number of years due to their chemical and topological versatility. As MOF research has progressed, highly functionalised materials have become desirable for specific applications, and in many cases the limitations of direct synthesis have been realised. This has resulted in the search for alternative synthetic routes, with postsynthetic modification (PSM), a term used to collectively describe the functionalisation of pre-synthesised MOFs whilst maintaining their desired characteristics, becoming a topic of interest. Advances in the scope of reactions performed are reported regularly; however reactions requiring harsh conditions can result in degradation of the framework. Zirconium-based MOFs present high chemical, thermal and mechanical stabilities, offering wider opportunities for the scope of reaction conditions that can be tolerated, which has seen a number of successful examples reported. This microreview discusses pertinent examples of PSM resulting in enhanced properties for specific applications, alongside fundamental transformations, which are categorised broadly into covalent modifications, surface transformations, metalations, linker and metal exchange, and cluster modifications.

1. Introduction

Metal-organic frameworks (MOFs)[1] are multidimensional materials containing metal ions or metal ion clusters that are connected by bridging multidentate organic ligands. The connectivity of these constituents into repeating, ordered structures typically imparts permanent porosity that is advantageous for various applications, including gas capture and storage,[2] catalysis[3] and drug delivery.[4] MOFs are routinely obtained via direct synthetic routes,[5] however postsynthetic modification (PSM) of MOFs – carrying out chemical transformation[6] or exchange on pre-synthesised materials[7] – has emerged as a powerful route to introduce functionality into MOFs. Indeed, in many cases, PSM is the only method by which certain moieties can be incorporated into MOFs without affecting the underlying structure. The tolerance of MOFs linked by Zr^{IV}-based clusters[8] towards harsh chemical[9] and mechanical[10] conditions makes them ideal platforms for introducing functionality by PSM, and this microreview will focus on the diverse range of both chemical transformations and modification protocols used to prepare materials with applications in mind.

[a] *WestCHEM, School of Chemistry, The University of Glasgow, University Avenue, Glasgow G12 8QQ, UK*
E-mail: Ross.Forgan@glasgow.ac.uk
www.forganlab.com
ORCID(s) from the author(s) for this article is/are available on the WWW under http://dx.doi.org/10.1002/ejic.201600394.

Ross Marshall is from South West Scotland and graduated from the University of Glasgow in 2013 with a BSc (Hons) in Chemistry. Ross performed his final year research project under the supervision of Dr Ross Forgan, before joining The Forgan Group as a PhD student. He is currently in the third year of his PhD, where he carries out research into the synthesis, characterisation and postsynthetic modification of Zr and Hf MOFs.

Dr Ross Forgan is a Royal Society University Research Fellow and Reader in the School of Chemistry at the University of Glasgow. After receiving MChem. (Hons) and PhD degrees from the University of Edinburgh in 2004 and 2008, under the supervision of Prof Peter Tasker, he spent three years as a postdoctoral researcher in the group of Prof. Sir J. Fraser Stoddart at Northwestern University, USA. In 2011 he returned to Scotland as a postdoctoral researcher in the group of Prof Lee Cronin at the University of Glasgow, and took up his current independent position in 2012. His research group is interested in the crystallisation and functionalisation of MOFs, as well as their materials properties and biomimetic applications.

Since the discovery of the UiO-66 series of MOFs by Lillerud et al. in 2008,[11] wherein $Zr_6O_4(OH)_4$ octahedral secondary building units (SBUs) link twelve linear dicarboxylate linkers each in three dimensions to form a highly porous network, a number of further Zr MOFs have been characterised, with most based on this Zr_6 SBU (Figure 1a and b).[8,12] Interpenetrated analogues of the UiO-66 series are known,[13] while the MIL-140 series of MOFs are also linked by dicarboxylates, but connected by one-dimensional Zr-oxide chains to form structures with one-dimensional porous channels.[14] Trigonal tricarboxylate ligands have been shown to link lower connectivity Zr_6 SBUs capped by solvents and/or monocarboxylates into two[15] and three[16] dimensional frameworks (Figure 1c). Planar tetracarboxylates can also be linked by derivatives of the Zr_6 SBU into highly porous frameworks, for example, tetrakis(4-carboxyphenyl)porphyrin (PCN-222, MOF-545, Figure 1d)[17] and 1,3,6,8-tetrakis(*p*-benzoate)pyrene (NU-1000),[18] while a twelve-connected Zr_8O_6 SBU has also been observed in a porphyrin-based system.[19] Tetrahedral tetracarboxylates have also been linked by Zr_6 SBUs of varying connectivities into three dimensional networks.[16b,20] Recently, Zr MOFs have been prepared using 1,2,3-trioxobenzene units as coordinating components in linear ligands, for example MIL-163, with one dimensional Zr–O chains linking the organic moieties.[21]

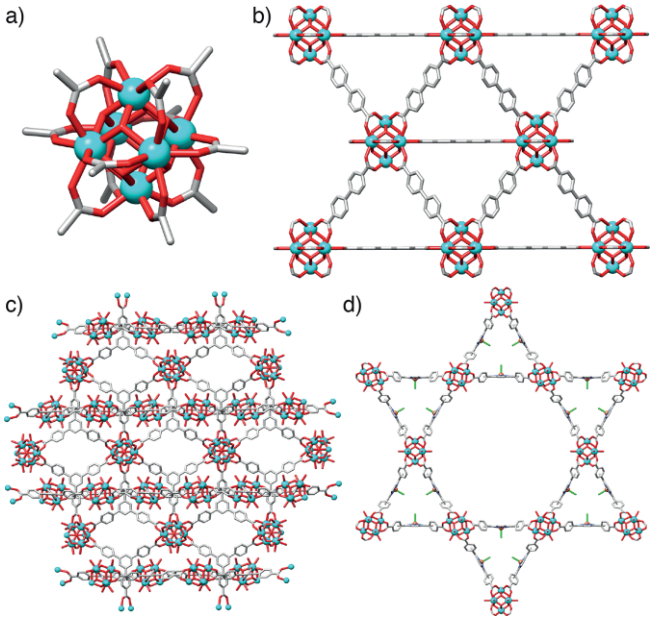

Figure 1. a) The $Zr_6O_4(OH)_4(RCO_2)_{12}$ secondary building unit, derivatives of which link the majority of Zr MOFs. b) Representation of the solid-state structure of $[Zr_6O_4(OH)_4(bpdc)_6]_n$, where bpdc = biphenyl-4,4′-dicarboxylate, commonly known as UiO-67. c) Representation of the solid-state structure of $[Zr_6O_4(OH)_4(btb)_6(OH)_6(H_2O)_6]_n$, where btb = benzene-1,3,5-tribenzoate. d) Representation of the solid-state structure of $[Zr_6(OH)_8(FeCl\text{-}TCPP)_2]_n$, where TCPP = tetrakis(4-carboxyphenyl)porphyrin, commonly known as PCN-222-Fe. Redrawn from CCDC depositions 1441659, 1000802 and 893545, in turn.

The majority of these Zr MOFs exhibit a key common property – high chemical stability – being resistant to water,[9] acids[22] and bases.[9c,22b] Additionally, evidence is building that Zr MOFs also possess excellent mechanical stability and resistance to pressure.[10b,10d,10f] In concert, these stabilities make Zr MOFs prime candidates for application in diverse areas, and considerable efforts have focused on the incorporation of the functionalities required to carry out such applications, often through PSM.[23] In the following microreview, we will examine fundamental and pertinent examples of application-driven PSM of Zr MOFs, organised broadly by the following modification protocols: covalent transformation of pendant and integral functional groups, surface modification, metalation, linker exchange, metal exchange and modification of the inorganic cluster.

2. Pendant Covalent Functionalisation

The vast majority of reported postsynthetic modification protocols are based upon the reactivity of pendant functional moieties on the organic linker of the MOF, with amine groups often exploited due to the wealth of chemical transformations possible (Figure 2). The first amine containing Zr MOF, UiO-66-NH_2, with chemical composition $[Zr_6O_4(OH)_4(NH_2\text{-}bdc)_6]_n$ (where NH_2-bdc is 2-amino-1,4-benzenedicarboxylate) was described independently by Tilset[9c] and Cohen[24] in 2010. Both groups subsequently demonstrated the postsynthetic reactivity of the pre-installed amine handle through reactions with a variety of acid anhydrides, resulting in amide functionalised pores. The liquid phase reactions (chlorinated solvents, varying times) were followed by a number of experimental techniques, including FT-IR and ^1H NMR spectroscopy, which provide evidence of the percentage conversion, whilst PXRD was used to demonstrate retention of crystallinity during the modification, highlighting the high chemical stability of Zr MOFs. It was observed that the

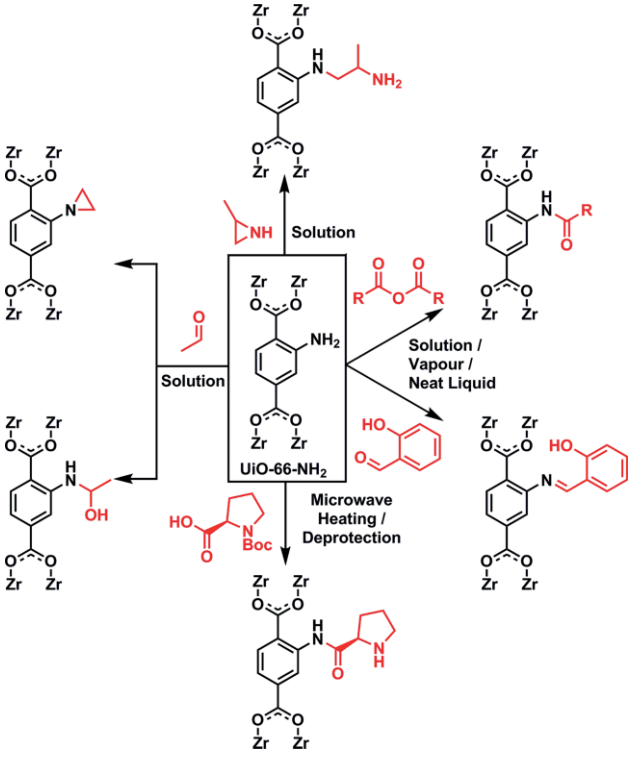

Figure 2. Examples of covalent postsynthetic modifications at the pendant amino units of UiO-66-NH_2.

greatest conversion was achieved with smaller anhydrides, likely due to pore size based restrictions.

In 2012, the PSM of UiO-66-NH_2 with acid anhydrides was extended to investigate the feasibility of vapour phase reactivity.[25] The authors report that the vapour method provides access to the amide modified MOF with improved conversions in reduced timescales. Aside from acid anhydrides, the reactivity of UiO-66-NH_2 with vapour phase salicylaldehyde was also demonstrated, resulting in an imine functionalised MOF. Although only modest conversion was achieved, this still outperformed the corresponding liquid phase reaction (ca. 29 % vs. 10 %) and demonstrates the high chemical stability of these types of frameworks.

In a later report, UiO-66-NH_2 reactivity was investigated through reaction with neat reagents, with relatively harsh conditions (100 °C) employed compared to previous work.[26] PSM of UiO-66-NH_2 with acetic anhydride was successfully demonstrated using this method, achieving 98 % conversion in as little as 10 minutes. The authors report that PSM with carboxylic acids did in some cases leads to decomposition of the framework, postulating that this is due to postsynthetic ligand exchange (see Section 6) owing to the free coordinating groups present on the reactive species. A study of UiO-66-NH_2 by Yaghi et al. suggested,[27] through solid state ^{15}N NMR spectroscopy measurements, that the MOF is actually comprised of both the free amine (NH_2-bdc) and ammonium chloride ($NH_3^+Cl^-$-bdc) ligands in a 2:1 ratio. PSM with acetaldehyde was subsequently investigated, resulting in conversions of up to 70 %, although both the hemiaminal and aziridine products were obtained, representing the kinetic and thermodynamic products respectively, and a further heating process could alter their relative ratios. These early reports have therefore provided the foundations detailing the feasibility of potential transformations on the amine handle of UiO-66-NH_2, although recent attention has focused on improving the materials properties, to enable their successful use in desired applications.

Wang et al. studied the PSM of UiO-66-NH_2 with 2-methylaziridine, yielding the corresponding MOF containing alkylamine lined pores in 28 % yield.[28] It was found that the modified material was an efficient catalyst for Knoevenagel condensations, as the alkylamine is able to successfully activate the aldehyde by forming an imine. In a typical reaction between benzaldehyde and malonitrile at room temperature in toluene, the yield of the reaction was improved from 5 % to 97 % in the presence of UiO-66-NH_2 and the alkylamine tagged UiO-66-NH_2 respectively. The authors also report that IRMOF-3 – a Zn MOF containing NH_2-bdc – does not withstand the postsynthetic modification, highlighting the high chemical stability of Zr MOFs. Indeed, the alkylamine modified UiO-66-NH_2 catalyst can be recycled five times without a loss of activity.

The free carboxylic acid groups of amino acids/peptides enable them to be coupled with UiO-66-NH_2, resulting in covalent functionalisation of the MOFs with a number of substrates. *tert*-Butoxycarbamate (Boc) protected enantiopure amino acids/peptides were coupled with UiO-66-NH_2 using a microwave assisted coupling procedure to prevent racemisation of the peptide.[29] The microwave assisted procedure results in higher yields of modification; during the coupling of UiO-66-NH_2 with L-proline <2 % conversion was achieved using 96 hours of conventional heating at 37 °C, although 10 % conversion was observed when coupled using microwave heating at 80 °C for 20 min. The coupling of dipeptides with UiO-66-NH_2 was also investigated, although essentially no conversion was observed, likely due to size-based restrictions. Importantly, PXRD analysis of UiO-66-NH-Pro (the PSM product after Boc deprotection) reveals that the MOF is able to withstand the chemical conditions encountered during the modification/deprotection, suggesting that better conversion may be obtained if a Zr MOF bearing an amine group with larger pore size dimensions was used.

UiO-66-NH_2 has been subjected to PSM with methacrylic anhydride, resulting in 67 % conversion, evidenced from ^1H NMR spectra of HF digests of the MOF, which was also in good agreement with elemental analysis results.[30] The methacrylate functionality was then used in further transformations (Figure 3a), where the modified MOF nanoparticles were mixed with butyl methacrylate (BMA) and the photo initiator phenylbis(2,4,6-trimethylbenzoyl)phosphine oxide, and then irradiated with UV light for several minutes. This photoinduced postsynthetic polymerisation (PSP) process results in a square shaped polymer which can be peeled from the Teflon surface as a stand-alone membrane (Figure 3b).

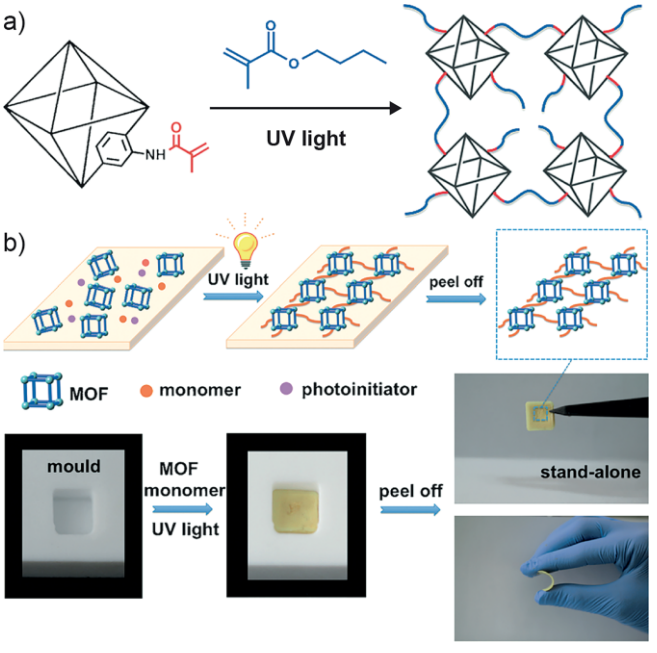

Figure 3. a) Postsynthetic polymerisation (PSP) of UiO-66-NH_2 functionalised with methacrylic anhydride. b) Representation of the PSP process used in the construction of stand-alone membranes, starting from UiO-66-NH_2. Reproduced (modified) with permission from ref.[30] Copyright (2015) Wiley-VCH.

CO_2 adsorption isotherms were used to prove the permanent porosity of the membrane, thus confirming that the MOF pores were not loaded with self-polymerised BMA polymer (PBMA). The CO_2 uptake capacity of the PSP membrane was found to exceed that of a blend of PBMA/MOF (both containing 20 % MOF), demonstrating the improved properties that the PSP membranes offer. Scanning electron microscopy (SEM) reveals that the initial modification with methacrylic anhydride is re-

quired, as the resulting membrane contains well-dispersed MOF nanoparticles. This was not true for a PSP membrane synthesised using non-modified UiO-66-NH_2 that formed conglomerates on the polymer surface. The PSP derived membrane was also investigated for its ability to separate Cr^{IV} ions from an aqueous solution, with a first cycle retention of 80 % and a separation capacity of 8 mg/g, which was a dramatic improvement compared with the other materials investigated.

Covalent modification of other pendant groups has also been investigated, with UiO-66-Br one of the first examples to be studied. UiO-66-Br was obtained by direct synthesis using 2-bromo-1,4-benzenedicarboxylate (Br-bdc) and then postsynthetic cyanation with CuCN in DMF produced UiO-66-CN, which the authors report to be difficult to obtain via direct synthesis.[31] The modification was explored via two synthetic routes, using either conventional or microwave heating, with microwave assisted cyanation resulting in conversion rates as high as 90 %. These results suggest that aryl bromide substitution may be a route to incorporation of a range of functional groups that may be difficult to incorporate during direct synthesis.

Zr MOFs containing substituted derivatives of the extended 4,4′-[1,4-phenylenebis(ethyne-2,1-diyl)]-dibenzoate ligand form interpenetrated UiO-66 analogues commonly known as porous interpenetrated zirconium organic frameworks (PIZOFs).[13] One such MOF containing pendant furan moieties was functionalised by Diels–Alder cycloadditions with a variety of substrates (Figure 4a); reaction with maleimide, *N*-methylmaleimide or *N*-phenylmaleimide resulted in conversions of 98 %, 99 % and 89 %, in turn, whilst modest *exo*/*endo* selectivities of 24 %, 16 % and 17 % were observed.[32]

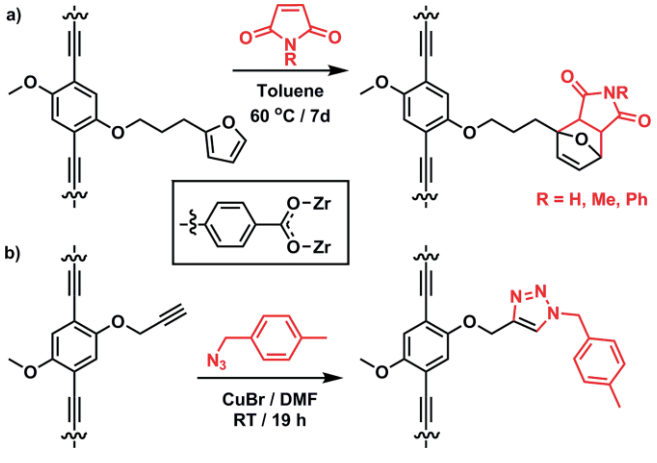

Figure 4. Schematic illustration of a) Diels–Alder cycloaddition, and b) Cu-catalysed azide-alkyne cycloaddition, both carried out postsynthetically on substituted interpenetrated Zr MOFs (PIZOFs).

The authors also report the copper-catalysed azide-alkyne cycloaddition (CuAAC) of another member of the series bearing pendant propargyl moieties. The alkyne units were treated with 4-methylbenzyl azide, using typical Cu^{I}-catalysed conditions, resulting in 98 % formation of the triazole product at room temperature (Figure 4b). This methodology can be viewed as an attractive route for the functionalisation of MOF pores under mild conditions, provided that the Cu^{I} can be efficiently removed after modification. Pendant alkyne functionalities have also been incorporated within a UiO-68 analogue containing 2′,5′-diethynyl-*p*-terphenyl-4,4″-dicarboxylate ligands.[33] The high porosity of the MOF enables the CuAAC reaction to proceed quantitatively with a number of substrates, namely azidoethane, azidoacetate and azidomethylbenzene, resulting in triazole functionalised MOFs with maintained porosity and crystallinity.

In a similar manner, other groups have focused on the synthesis of Zr MOFs containing pendant azide groups, which are likewise available for PSM by CuAAC. Zhou et al. reported the single crystal structures of a series of UiO-68 type MOFs containing *p*-terphenyl-4,4″-dicarboxylate ligands, bearing either two or four pendant methyl or azidomethyl functional groups on the central benzene ring.[34] By judiciously adjusting the molar ratios of the ligands in the synthetic mixture, mixed-ligand MOFs with azide loadings of 0, 25, 50, 75 and 100 % were obtained. The MOFs containing various azide loadings were treated with propargyl alcohol, as well as a variety of other alkyne substrates (Figure 5a). The introduction of nucleophilic hydroxyl groups results in improved CO_2/N_2 selectivity performances when compared to the parent azide containing MOFs. In another report, the UiO-68 type MOF containing two pendant azide groups was postsynthetically modified with a tetra-acetylene crosslinker under typical CuAAC conditions. The acetylene containing compound was observed to bridge the organic ligands of the MOF, resulting in the formation of a cross linked MOF (CLM) whilst retaining crystallinity. The authors then selectively destroyed the metal coordination bonds within the CLM by reacting with acidic HCl solutions. The resulting poly-

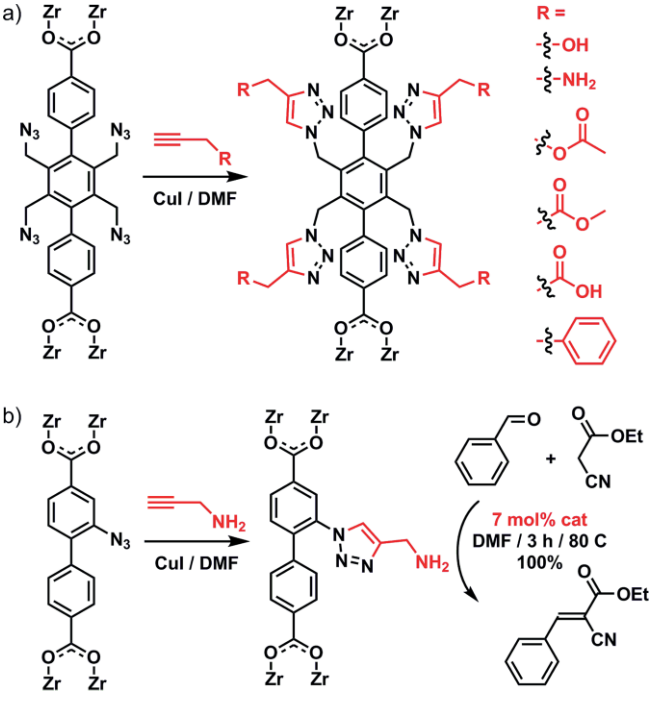

Figure 5. a) Tetra-azido modified Zr MOFs undergoing Cu-catalysed azide-alkyne cycloaddition with a variety of substrates. b) Functionalisation of UiO-67-N_3 with propargylamine to produce a catalyst for the Knoevenagel condensation between benzaldehyde and ethyl cyanoacetate.

mer gels were insoluble and retained the shape of the original crystals, hence the MOFs were able to act as a template towards polymer gels with pre-designed architectures.[35]

UiO-67-N_3, which contains 2-azidobiphenyl-4,4′-dicarboxylate, has been prepared, although the reaction temperature had to be reduced to 80 °C as conventional synthetic methods (140 °C) resulted in thermal cyclisation of the ligand to 9*H*-carbazole-2,7-dicarboxylate in situ.[36] This phenomenon also results in a poor thermal stability of the MOF, as thermal cyclisation results in a bent ligand geometry that cannot be accommodated by the framework, resulting in collapse of the overall network structure. Low chemical stability was observed, with crystallinity lost when the MOF was immersed in common organic solvents, however framework integrity was retained in DMF, allowing CuAAC reactions with alkyne substrates to be performed. Quantitative conversion was observed when the MOF was modified with methyl propiolate, 3-butyn-1-ol and propargylamine, and interestingly the modified products demonstrated improved chemical and thermal stabilities when compared with the parent framework. The pendant amino group of the propargylamine modified framework was an efficient catalyst for the Knoevenagel condensation between benzaldehyde and ethyl cyanoacetate (Figure 5b), with the MOF sufficiently stable to be reused for multiple catalytic cycles.

UiO-68-allyl, comprising 2′,5′-bis(allyloxy)-*p*-terphenyl-4,4″-dicarboxylate ligands, was synthesised and subject to postsynthetic modification by thiol-ene radical addition, through near quantitative reaction of the allyl moiety with ethanethiol under UV light in the presence of 2,2-dimethoxy-2-phenylacetophenone as a photoinitiator (Figure 6).[37] Thiol-ene and thiol-yne additions represent very useful routes to access functionalised MOFs, as they allow the mild insertion of a variety of functional groups across unsaturated double and triple bonds, although success thus far has been limited to pendant groups.[38]

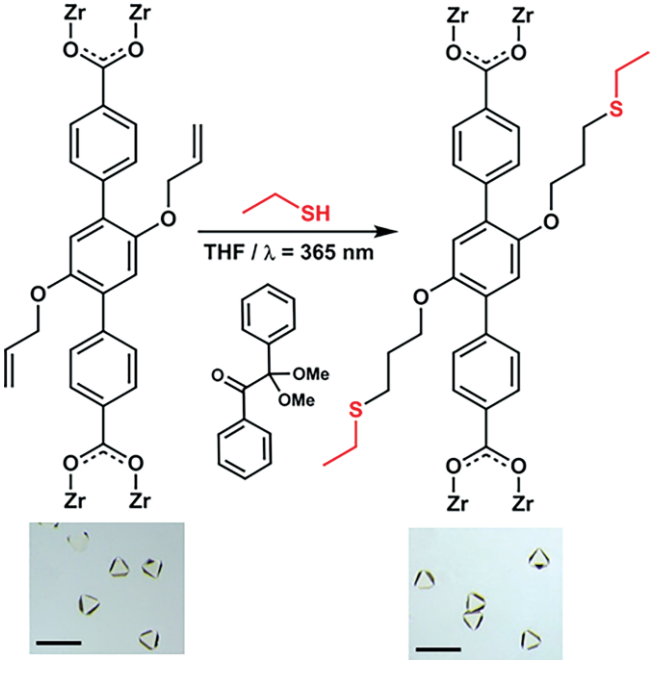

Figure 6. Schematic illustration of the thiol-ene radical addition of ethanethiol to UiO-68-allyl, with the single crystal images highlighting that the crystals remain intact during the transformation (scale bar = 200 μm). Reproduced (modified) with permission from ref.[37] Copyright (2015) Elsevier.

MOFs bearing pendant carboxylic acid or sulfonic acid groups are of broad interest as they have been shown to result in improved characteristics including enhanced CO_2 selectivity[39] and proton conductivity.[40] These additional acidic groups provide further sites for attachment to metal ions, which in many cases disrupts direct MOF formation, and so introduction of acidic groups onto the backbone of the MOF has been investigated by a postsynthetic oxidation approach. To generate sulfonic acid moieties, UiO-66-$(SH)_2$ was synthesised directly from 1,4-dicarboxybenzene-2,5-dithiol, then the MOF was subjected to harsh chemical conditions: an aqueous 30 % H_2O_2 solution for oxidation of the thiol groups, followed by an acidic solution for protonation, resulting in quantitative conversion to UiO-66-$(SO_3H)_2$ (Figure 7a).[41] The postsynthetic process was completed in as little as 90 min, resulting in quantitative conversion, while PXRD was used to prove the retention of crystallinity of the MOF. Introduction of the acidic sulfonic groups greatly improved the hydrophilicity of the MOF, which was beneficial for proton conduction. UiO-66-$(SO_3H)_2$ demonstrated an excellent superprotonic conductivity of 8.4×10^{-2} Scm^{-1} at 80 °C and 90 % relative humidity, and an activation energy for proton transfer of 0.32 eV (Figure 7b). This is the highest reported value of protonic conductivity of MOFs and is comparable to the performance of Nafion, a perfluorinated polymer membrane that is the most effective polymer electrolyte known, and as such this material could potentially be incorporated into proton-exchange membrane fuel cells as an alternative energy technology.

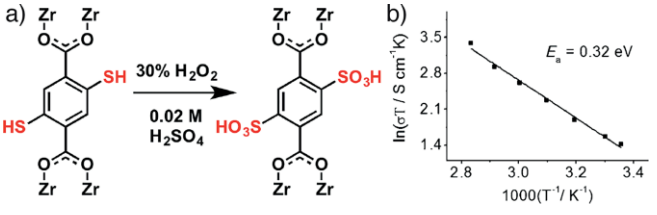

Figure 7. a) Schematic illustration of the postsynthetic oxidation of thiol units to form sulfonic acid groups. b) An Arrhenius plot of UiO-66-$(SO_3H)_2$ at 90 % relative humidity, revealing an activation of energy of 0.32 eV for proton conduction. Reproduced (modified) with permission from ref.[41] Copyright (2015) Wiley-VCH.

Clet et al. were however, able to successfully synthesise UiO-66-(CO_2H) and UiO-66-$(CO_2H)_2$, bearing one or two free carboxylic acid groups respectively within the pores, via a direct water-based synthetic route.[42] Interestingly it was found that heating the solids under vacuum results in formation of anhydride bridges between carboxylic acid groups on adjacent ligands, as evidenced by FT-IR and solid-state NMR spectroscopy. It was observed that samples containing increasing amounts of the anhydride bridges resulted in higher adsorption capacities for methane and carbon dioxide at 30 °C and 10 bar of the respective gas. Partial reversibility of the anhydride bridges was also observed when the samples were in contact with water vapour.

Redox processes have also been observed to occur postsynthetically in a single-crystal to single-crystal (SCSC) manner in UiO-68-$(OH)_2$, which contains 2′,5′-dihydroxy-*p*-terphenyl-4,4″-dicarboxylate ligands.[43] The ligand within the MOF could be oxidised in the solid phase from the diol to the quinone form, resulting in altered spectroscopic properties (Figure 8). The transformation was fully reversible, and it was observed that the transformation occurs on the outmost surface of the crystals and gradually diffuses inwards. Interestingly, the MOF could not be directly synthesised with the quinone based ligand, however incorporating these organic-based molecular switches into the solid phase may prove useful for applications such as memory storage or redox-based electronic devices.

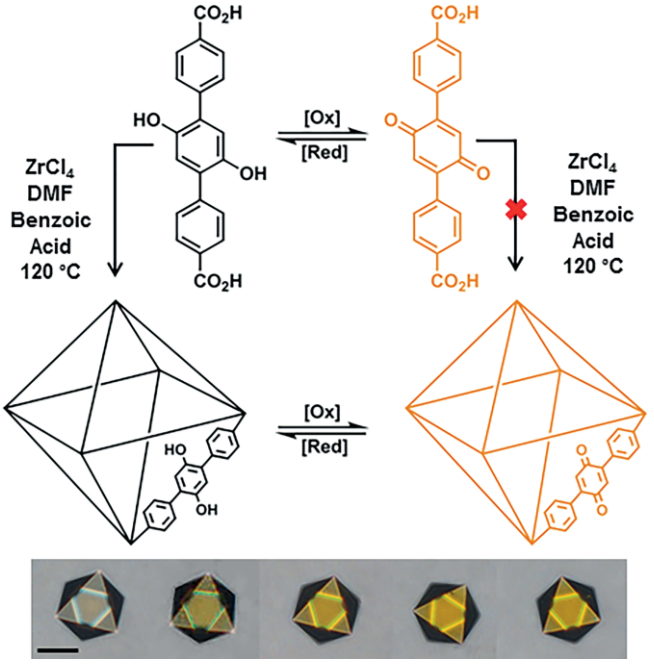

Figure 8. Schematic illustration of the redox switching behaviour of UiO-68-$(OH)_2$ to the quinone form, which was unable to be synthesised directly (scale bar = 50 μm). Reproduced (modified) with permission from ref.[43] Copyright (2015) American Chemical Society.

There has clearly been a significant drive to study the postsynthetic modification of pendant functionalities within Zr MOFs in a similar manner to earlier efforts focusing on the modification of other transition metal containing MOFs. The enhanced chemical and mechanical stabilities of Zr MOFs are advantageous, as the MOFs are tolerant of a wealth of harsh chemical conditions, meaning that facile access to the specialised modified materials facilitates their utilisation into desired applications.

3. Integral Covalent Modification

There are considerably fewer examples of postsynthetic modification of MOFs at integral linker sites rather than on pendant functional groups, likely as a consequence of the generally low reactivity of the largely structural components. The chemical stability of Zr MOFs means they can tolerate harsh reaction conditions, facilitating reactions directly on unfunctionalised aromatic rings. Bradshaw et al. showed that UiO-66 was stable in the presence of hydroxyl radicals in water to selectively form UiO-66-OH by PSM with no loss of crystallinity.[44] The ·OH radicals can be generated by UV-A irradiation of the superparamagnetic photocatalytic composite material γ-Fe_2O_3@SiO_2@TiO_2 or UV-C irradiation of aqueous H_2O_2 solutions, with the former method resulting in a higher hydroxylation yield (77 % vs. 41 % conversion, Figure 9), and both higher than achievable by postsynthetic exchange (see Section 6). Introduction of free hydroxyl units to MOFs by PSM is valuable, as they are often coordinated to metals during direct synthesis.

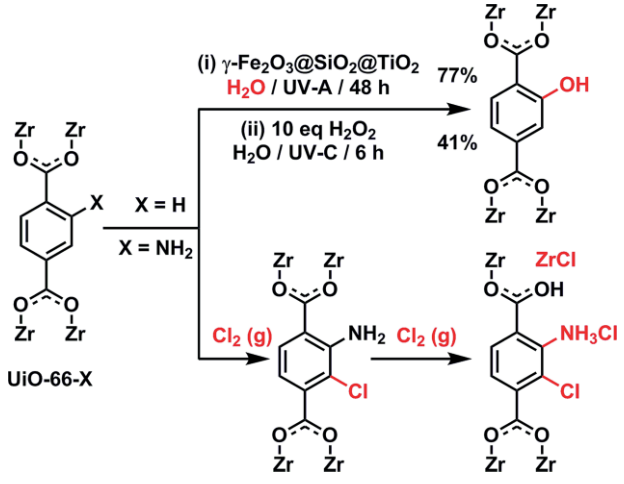

Figure 9. Conditions for postsynthetic hydroxylation and chlorination directly on the aromatic rings of UiO-66 and UiO-66-NH_2 respectively. Exposure of UiO-66-NH_2 to excess chlorine gas eventually results in its decomposition.

Similar chemical stability of UiO-66 in the presence of Cl_2 gas was demonstrated by DeCoste and Peterson, who showed that UiO-66-NH_2 underwent electrophilic aromatic substitution in the presence of chlorine to form UiO-66-NH_2-Cl.[45] Further exposure to chlorine resulted in eventual degradation of the MOF and pore collapse (Figure 9), but UiO-66-NH_2 exhibits a Cl_2 storage capacity of 124 % *w/w*, and is a candidate material for air purification.

It is also possible to carry out reactions at heteroatoms in ligand ring systems. Chen and Qian prepared the MOF known both as UiO-67(bipy) and MOF-867 – $[Zr_6O_4(OH)_4(bpydc)_6]_n$ where bpydc = 2,2′-bipyridine-5,5′-dicarboxylate – and methylated the nitrogen atoms of the bpydc linker with methyl triflate in 70 % yield. The generation of cationic pyridinium sites (the charges are balanced by nitrate counterions introduced during washing) means the material exhibits highly efficient removal of pollutant dichromate anions, $Cr_2O_7^{2-}$, from aqueous solution.[46]

The efficacy of reactions such as the Sonogashira and Heck couplings to link aromatic units means that many MOF linkers contain integral carbon–carbon double and triple bonds in their backbones. Forgan et al. have demonstrated that Zr MOFs possess the requisite mechanical stability[10d] to allow halogenation of integral unsaturated bonds of a series of materials, where the change in hybridisation of linker carbon atoms results in an overall mechanical contraction.[47] UiO-66 topology MOFs containing integral alkene, alkyne and butadiyne units (Figure 10a) were quantitatively brominated by immersing them in

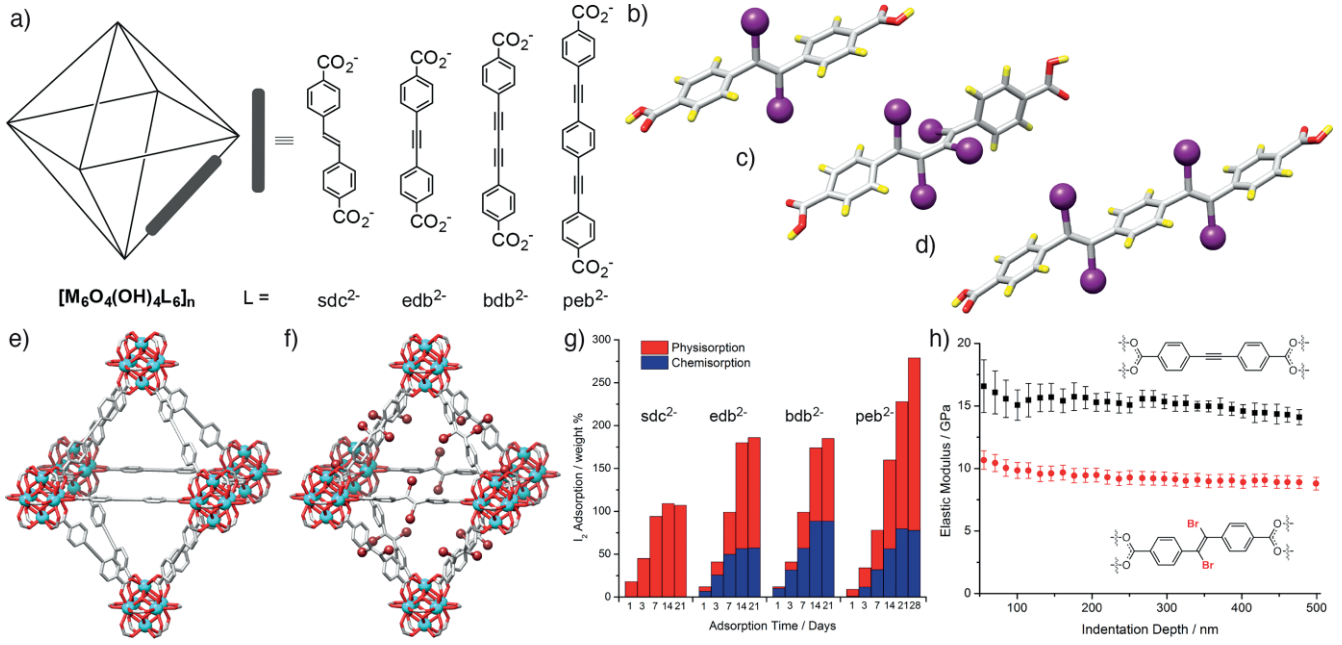

Figure 10. a) Schematic of Zr MOFs that have been halogenated at unsaturated C–C bonds. Crystal structures of b) *trans*-edb–I_2–H_2, c) *trans*,*trans*-bdb–I_4–H_2, and d) *trans*,*trans*-peb–I_4–H_2 isolated from iodinated Zr MOFs showing exclusive *trans* stereochemistry. Redrawn from CCDC depositions 1400977, 1443200 and 1443201, in turn. Single-crystal to single-crystal transformation of e) $[Zr_6O_4(OH)_4(edb)_6]_n$ to f) $[Zr_6O_4(OH)_4(edb\text{-}Br_2)_6]_n$, redrawn from CCDC depositions 1062508 and 1062510. g) Iodine uptake of the MOFs described in part a). Reproduced with permission from ref.[48] Copyright (2016) Wiley-VCH. h) Comparison of elastic moduli vs. indentation depth for $[Zr_6O_4(OH)_4(edb)_6]_n$ and $[Zr_6O_4(OH)_4(edb\text{-}Br_2)_6]_n$ measured by nanoindentation. Reproduced with permission from ref.[10c] Copyright (2016) Royal Society of Chemistry.

chloroform solutions containing Br_2, with no decrease in porosity or crystallinity.[48] As the linkers have restricted dynamic motion when bound within the MOFs, the transformations are stereoselective, yielding exclusively *trans*-dihaloalkene and *meso*-dihaloalkane units (Figure 10b–d). The MOFs have sufficient mechanical stability to allow single-crystal to single-crystal transformations to occur, with full structural characterisation of the halogenated products possible (Figure 10e,f), while their chemical stability towards both halogens and water means that bromohydrination – the installation of one bromine and one hydroxyl unit across an unsaturated bond – can also be carried out. Halogenation was extended to chemisorption of iodine from the vapour phase by addition across multiple bonds, which could have great significance in the sequestration of radioactive iodine from the nuclear industry. The interpenetrated Zr MOF $[Zr_6O_4(OH)_4(peb)_6]_n$, where peb is the bis-alkyne ligand 4,4′-[1,4-phenylenebis(ethyne-2,1-diyl)]-dibenzoate, can adsorb 279 % *w*/*w* of iodine by a combination of chemisorption across the alkyne units and physisorption in the large pores (Figure 10g).[48] The change in hybridisation of the carbon atoms in the linkers on postsynthetic halogenation also results in a change in mechanical compliance, which can be measured by single crystal nanoindentation. For example, the MOF $[Zr_6O_4(OH)_4(edb)_6]_n$, a UiO-66 topology material where edb = 4,4′-ethynylenedibenzoate, has a Young's modulus of 15.1 (±0.8) GPa, which decreases on bromination to 9.3 (±0.6) GPa as a consequence of the increased flexibility of the linker (Figure 10h).[10c]

4. Surface Functionalisation

Limiting postsynthetic modification to the outer surfaces of MOF particles has been shown to induce a number of attractive properties related to both stability and application.[49] A small group of surface modified Zr MOFs have been prepared largely from amino-tagged UiO-66 derivatives, using modifying agents that are too large to penetrate the pores of the MOF and so limit PSM to the particle surfaces. UiO-66-NH_2 can be surface coated with a porous organic polymer by carrying out a Sonogashira coupling-based polymerisation in the presence of the MOF.[50] The resultant materials exhibited considerable hydrophobicity and highly efficient removal of organic compounds from water. The mode of attachment of the polymer to the MOF is presumably noncovalent – attempts to functionalise UiO-66-I in the same way were unsuccessful – so this may be a case of the MOF acting simply as a template for polymer formation. Sada and Kokado attached poly(*N*-isopropylacrylamide) (PNIPAM) chains terminated with *N*-hydroxysuccinimide (NHS) activated esters to UiO-66-NH_2 by amide coupling (Figure 11). The temperature responsive mechanical behaviour of PNIPAM – it collapses into a globule formation at higher temperatures – allowed the researchers to control access to the pores, resulting in stimuli-responsive release of drug molecules from UiO-66-PNIPAM when temperatures were lowered.[51]

Rosi and Albenze showed that UiO-66-NH_2 had appropriate chemical stability to allow amide formation by reaction with acid chlorides, despite HCl being a byproduct of the reaction,

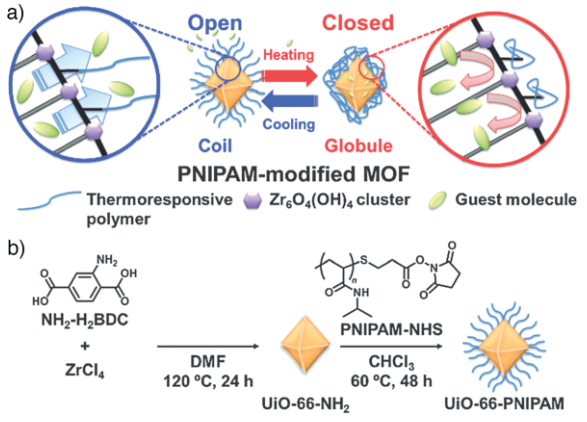

Figure 11. a) Schematic illustrating temperature control of pore openings in PNIPAM-modified UiO-66-NH_2. b) The postsynthetic surface modification procedure to install PNIPAM on the surface of UiO-66-NH_2. Reproduced with permission from ref.[51] Copyright (2015) Royal Society of Chemistry.

and added alkyl and aryl units to the MOF surface.[52] These hydrophobic moieties allow greater integration into Matrimid polymers, generating mixed membranes with improved stabilities and enhanced gas uptake properties.

Modifying the surfaces of nanoparticles is a well-established technique for drug delivery, and an area in which MOFs show great promise.[4] Lin has demonstrated that nanoparticles of UiO-68-NH_2, an analogue of UiO-66-NH_2 with an extended 2′-amino-*p*-terphenyl-4,4′′-dicarboxylate linker, can be functionalised on the surface with small interfering RNA (siRNA) molecules by coordination between their phosphate backbones and external Zr^{4+} cations, which have a great affinity for phosphate.[53] In this example, it is the MOF which protects the surface moiety; when MOFs loaded with a cisplatin prodrug and modified with siRNA were introduced to cisplatin-resistant cancer cells, the siRNA was not only protected from nuclease degradation, but showed enhanced cellular uptake and gene silencing, dramatically enhancing chemotherapeutic efficiency. Mirkin also took advantage of zirconium's affinity for phosphate by surface modifying a number of UiO-66 series MOFs with the phospholipid 1,2-dioleoyl-*sn*-glycero-3-phosphate (DOPA), through exposure of the MOFs to a chloroform solution of the sodium salt of DOPA to induce coordination.[54] The location of the DOPA molecules was confirmed to be on the surface of the MOFs by a fluorescent dye, while surface coverage could be easily controlled. The hydrophobic surface ligand allowed the usually hydrophilic MOF to be colloidally dispersed in chloroform, with no detrimental effect on crystallinity or porosity.

Mirkin also showed that oligonucleotides could be covalently attached to the surface of UiO-66-N_3, utilising strain-promoted alkyne-azide cycloaddition (SPAAC) to "click" dibenzylcyclooctyne-substituted DNA strands of 20 nucleobases in length to the MOF (Figure 12).[55] Radiolabelling confirmed modification occurred at the surface only, and the DNA modified MOF particles showed enhanced stability and cellular uptake.

It is clear that surface modified MOFs have great potential in biomedicine, but current methods rely entirely on the surface ligand being too large to penetrate the pores of the MOF. Future modification protocols could focus on introducing functional groups solely at the surfaces of the MOFs, which would allow a wider variety of MOFs to be functionalised.

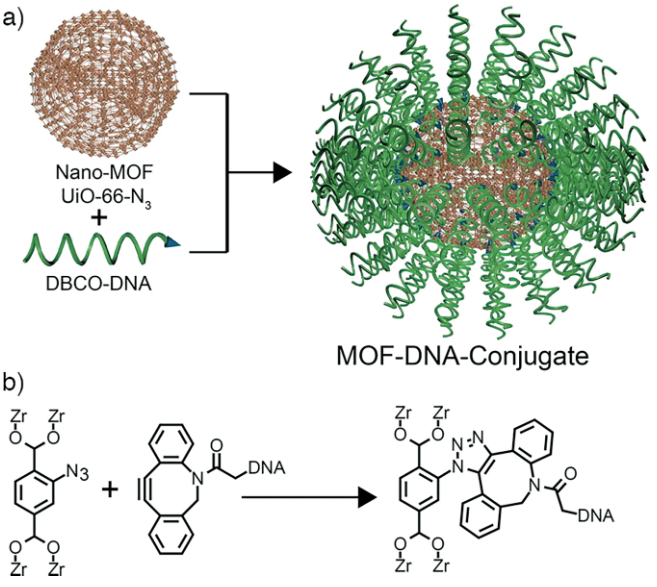

Figure 12. a) Schematic showing the surface modification of UiO-66-N_3 nanoparticles with DNA by b) postsynthetic strain-promoted alkyne-azide cycloaddition with dibenzocyclooctyne (DBCO) functionalised oligonucleotide strands. Reproduced (modified) with permission from ref.[55] Copyright (2015) American Chemical Society.

5. Postsynthetic Metalation

PSM can also be achieved by incorporation of secondary metal ions into pre-synthesised frameworks. UiO-66, containing bdc ligands, was postsynthetically metalated with $Cr(CO)_6$ via thermal decomposition of the metal carbonyl compound to afford η^6-arene-$Cr(CO)_3$ units grafted onto the benzene-based ligands.[56] Photoinduced substitution of one of the carbonyl moieties with a nitrogen molecule was highlighted, which the authors suggest may hold potential in small molecule fixation and activation. One route that has been investigated for incorporation of alkali metal cations into UiO-66 type MOFs is to include pendant $-SO_3H$[57] or $-CO_2H$[58] groups on the ligands. Using alkali metal hydroxide solutions it was demonstrated that a range of cations (Li^+, Na^+ and K^+) could be introduced into the framework. The resultant materials were investigated for their CO_2 storage capacities, as well as their CO_2/N_2 selectivities. One of the reported materials containing sodium ions, UiO-66-$(CO_2Na)_2$, was found to have a CO_2/N_2 selectivity of 99.6, a significant improvement compared with a selectivity of 66.9 obtained for the unfunctionalised UiO-66-$(CO_2H)_2$.

Zr MOFs possessing metal chelation sites have received appreciable amounts of interest for a number of applications, with one of the most widely studied materials being UiO-67(bipy), also known as MOF-867, composed of 2,2′-bipyridine-5,5′-dicarboxylate bridging ligands.[59] The structure of UiO-67(bipy) is very similar to that of the well-known UiO-67, with the addition of the accessible bipy sites lining the MOF pores, as the hard Zr^{IV} cations are not coordinated during synthesis. The high

chemical stability of Zr MOFs enables UiO-67(bipy) to undergo metalation in a single-crystal to single-crystal manner (Figure 13a).[60] Postsynthetic metalation can be achieved with a range of substrates, allowing the insertion of CuCl, $CuCl_2$, $CoCl_2$, $FeBr_2$ and $Cr(CO)_6$ within the framework by exposing the MOF to either solutions or vapour (in a closed system) containing the transition metal source. Postsynthetic metalation of the framework occurs almost quantitatively and interestingly the symmetry of UiO-67(bipy) is altered during the process, with the space group changing from $Fm\bar{3}m$ to $Pa\bar{3}$, as a direct result of the ordering of the metalated linkers.

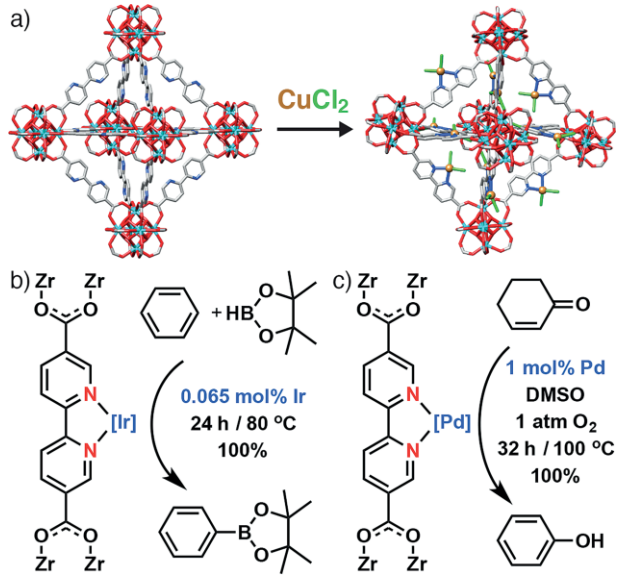

Figure 13. a) Representations of the crystal structures of UiO-67(bipy) which can be metalated to UiO-67(bipy)$CuCl_2$ in a single-crystal to single-crystal manner. Redrawn from CCDC depositions 968930 and 1042965, respectively. b) Catalytic arene borylation by UiO-67(bipy)Ir. c) Catalytic dehydrogenation of cyclohexanones by UiO-67(bipy)Pd.

Metalation with $[Ir(COD)_2]BF_4$ (COD = 1,5-cyclooctadiene) results in less than 10 % occupancy of Ir at the bipyridine sites, however the resulting material was found to be an efficient and recyclable catalyst for borylation of a number of arene precursors (Figure 13b). Several other reports have focused on the postsynthetic metalation of UiO-67(bipy) for catalytic applications. In 2014, Lin et al. postsynthetically metalated UiO-67(bipy) by soaking the MOF in either a tetrahydrofuran or dimethyl sulfoxide solution of $[Ir(COD)(OMe)]_2$ or $[Pd(CH_3CN)_4][BF_4]$ respectively at room temperature, resulting in an Ir loading of 30 % and a Pd loading of 24 %.[61] The metalated frameworks were again proven to be highly efficient single site heterogeneous catalysts; C–H borylation of arenes and intramolecular *ortho*-silylation of benzylic silyl ethers to benzoxasiloles using UiO-67(bipy)Ir, and dehydrogenation of substituted cyclohexanones to phenols using UiO-67(bipy)Pd (Figure 13c) were demonstrated. The catalytic activities of the metalated MOFs were compared to the homogeneous catalysts, and in the silylation reaction, UiO-67(bipy)Ir was found to be at least 1250 times more active. These high activities coupled with the recyclability of the MOF catalysts, due to their high stabilities, makes them prime candidates for use in catalytic technologies.

Cohen et al. investigated the catalytic activity of a mixed ligand UiO-67 type MOF containing both biphenyl-4,4′-dicarboxylate (bpdc) and 2,2′-bipyridine-5,5′-dicarboxylate (bpydc) ligands in a 3:1 ratio. Postsynthetic metalation of the mixed-ligand MOF with $Ru(bipy)_2Cl_2$ resulted in a Ru loading of ca. 10 %, although this could be controlled by alteration of the reaction time.[62] The resulting MOF was found to be an efficient and recyclable photocatalyst for the aerobic oxidative hydroxylation of arylboronic acids (Figure 14a).

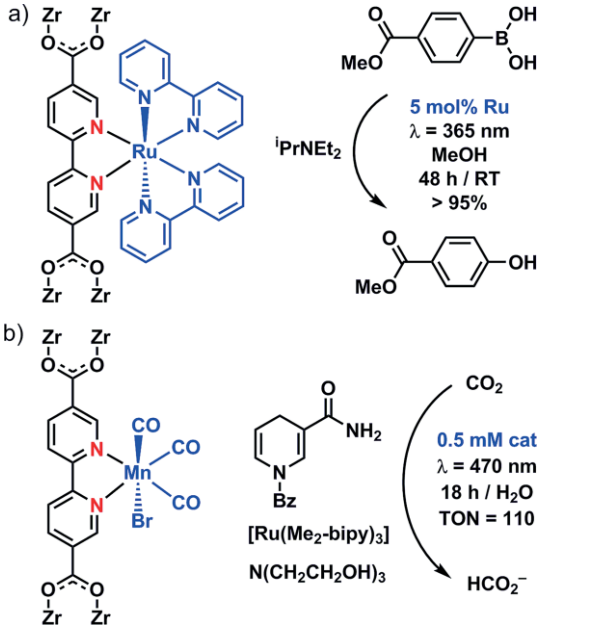

Figure 14. Postsynthetically metalated UiO-67 type MOFs containing either photocatalytically active a) ruthenium or b) manganese centres that were studied for the oxidative hydroxylation of arylboronic acids or for the reduction of CO_2 to formate respectively.

Another mixed ligand UiO-67 type MOF, this time containing a 1:1 ratio of the bpdc and bpydc ligands, was metalated with bromopentacarbonylmanganese(I) $[Mn(CO)_5Br]$. Inductively coupled plasma-optical emission spectroscopy (ICP-OES) confirmed that 76 % of the bpydc ligands were successfully metalated with the Mn^I photocatalyst, while direct synthetic attempts under comparatively harsh conditions were unsuccessful due to decomposition of the Mn^I complex.[63] The photocatalytic reduction of CO_2 to formate was investigated using the Mn^I incorporated MOF, in the presence of $[Ru(dmb)_3]^{2+}$ (dmb = 4,4′-dimethyl-2,2′-bipyridine) as a redox photosensitiser and 1-benzyl-1,4-dihydronicotinamide as a sacrificial reducing agent, and it was found that the overall turnover number and selectivity was higher than the homogeneous catalytic systems (Figure 14b).

UiO-67(bipy) has been investigated for alternative applications including luminescent sensing of transition metal ions, where the MOF acts as both the chelator and the fluorescence reporter.[64] Of the range of transition metal ions investigated during the study, Mn^{II}, Fe^{II}, Fe^{III}, Cd^{II}, Co^{II}, Cu^{II}, Ni^{II} and Zn^{II} were all found to quench the MOF's intrinsic luminescence, with the most sensitive detection observed for Fe^{III}, at a detection limit of 3.2 parts per billion. UiO-67(bipy) demonstrated an increased

sensitivity for all of the metal ions compared with the free bipy ligand. Alternatively, sensing of volatile organic compounds has been performed using Eu@UiO-67(bipy) composites which contain a small amount of chelated Eu (2.1 %) that is introduced postsynthetically by immersing the MOF in a methanolic solution containing $EuCl_3$.[65] Using the MOF it is possible to discriminate between the presence of related volatile organic compounds with similar structures and physical properties by a dual orthogonal readout system that is dependent on both luminescence quantum yield and ratiometric emission intensity.

Zr MOFs containing alternative metal chelation sites have been studied, with a catechol functionalised UiO-66 MOF recently synthesised and investigated for postsynthetic metalation and subsequently heterogeneous catalytic activity.[66] UiO-66-CAT could not be prepared directly, rather the catechol bearing ligand, 2,3-dihydroxy-1,4-benzenedicarboxylate, was introduced postsynthetically either via postsynthetic deprotection (PSD) or postsynthetic exchange (PSE). Briefly, PSE is a process where the solid phase MOF undergoes ligand exchange, resulting in incorporation of secondary ligands by substitution of the parent ligand (described in detail in Section 6) while PSD describes the cleavage of protecting groups using external stimuli to reveal the desired functionality. Subsequently, postsynthetic metalation with either iron, in the form of $Fe(ClO_4)_3$ or $Fe(CF_3SO_3)_3$, or chromium (K_2CrO_4) yielded unprecedented metal-monochelato species containing coordinatively unsaturated metal centres. UiO-66-CAT-Cr was found to be a highly efficient catalyst for the oxidation of alcohols to ketones even with very low chromium loadings (0.5–1.0 mol-%, Figure 15). The versatility of the catalyst was proven during the oxidation of eight different substrates, which was observed to occur almost quantitatively in many cases. The high chemical stability of UiO-66-CAT-Cr allows the MOF to be recycled for a number of catalytic cycles, further increasing its potential for use in catalytic applications.

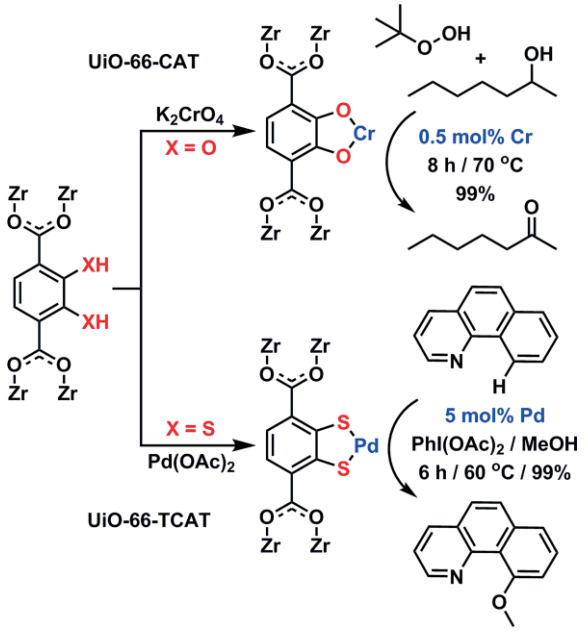

Figure 15. Schematic illustration highlighting metalations of UiO-66-CAT with Cr and UiO-66-TCAT with Pd, yielding excellent catalysts for oxidation and C–H activation, respectively.

In a further study, UiO-66-CAT was postsynthetically metalated with gallium [aqueous $Ga(NO_3)_3(H_2O)_x$ solution] to afford UiO-66-CAT-Ga.[67] The three metalated monochelato MOFs (UiO-66-CAT-M, M = Cr^{III}, Fe^{III} or Ga^{III}) were examined for their catalytic activities during the photocatalytic reduction of CO_2 to formate, however the Fe material did not demonstrate any catalytic activity as the redox potential for Fe^{III} (0.77 V vs. standard hydrogen electrode) is not suitable for CO_2 reduction. Of the remaining two metalated materials, it was found that UiO-66-CAT-Cr demonstrated greater catalytic activity, with turnover numbers calculated as 11.22 and 6.14 for UiO-66-CAT-Cr and UiO-66-CAT-Ga, respectively. A very similar analogue, UiO-66-TCAT, was synthesised by PSE of UiO-66 with 1,4-dicarboxybenzene-2,3-dithiol to afford a mixed ligand MOF containing open sulfur metal chelating sites.[68] UiO-66-TCAT was postsynthetically metalated with $Pd(OAc)_2$ (CH_2Cl_2 solution) to afford a dark brown solid containing accessible and coordinatively unsaturated Pd centres. Strong Pd–S bonds enable this MOF to be an efficient and recyclable catalyst for regioselective sp^2 C–H oxidation, with conversion to ether or aryl halide functionalities demonstrated (Figure 15).

A salicylaldimine based Zr MOF (sal-MOF) containing terphenyl based bridging ligands with pendant salicylaldimine functionality similar to UiO-68, was synthesised and postsynthetically metalated with tetrahydrofuran solutions containing cobalt ($CoCl_2$) or iron ($FeCl_2{\cdot}4H_2O$) to afford active single site solid catalysts for olefin hydrogenation, christened sal-Co-MOF and sal-Fe-MOF, respectively (Figure 16).[69] The spatial arrangement of the metal-salicylaldimine units within the MOF prevents oligomerisation, in contrast to homogeneous analogues that oligomerise, causing them to be inactive olefin hydrogenation catalysts. Impressively, during the hydrogenation of 1-octene under optimised conditions, sal-Fe-MOF had a turnover number of 1.45×10^5. The high catalytic activity of the sal-Fe-MOF is also recognised through the successful hydrogenation

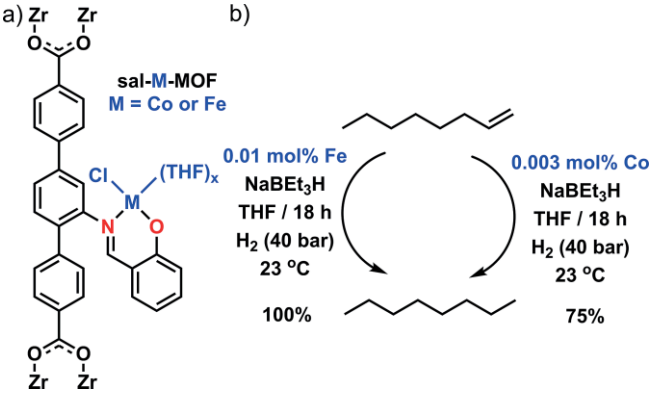

Figure 16. a) Representation of the salicylaldimine containing MOF, sal-M-MOF, with the metal binding site (both Co and Fe were investigated) highlighted, alongside b) summarised conditions for the catalytic hydrogenation of 1-octene using the sal-M-MOFs.

of a range of chemically and structurally varied terminal alkenes, while functional groups such as aldehydes, ketones and esters can be tolerated.

Lin and co-workers have utilised extended UiO-type MOFs containing longer ligands with potential metal docking sites, resulting in increased pore openings which offers opportunities for a wider range of substrates for catalytic investigations. An extended dicarboxylate ligand containing phenanthroline units was incorporated into a mixed ligand Zr MOF, alongside 4,4′-bis(carboxyphenyl)-2-nitro-1,1′-biphenyl (≈ 1:2 ratio) which offers reduced steric bulk, with the MOF named mPT-MOF (Figure 17a).[70] Postsynthetic metalation with $[Ir(COD)(OMe)]_2$ successfully produced mPT-MOF-Ir, a highly active catalyst for three different C–H activation reactions, specifically tandem hydrosilylation/*ortho*-silylation of aryl ketones and aldehydes (Figure 17b), tandem dehydrocoupling/*ortho*-silylation reactions of *N*-methylbenzylamines (Figure 17c), and borylations of aromatic C–H bonds. It was found that the mixed ligand MOFs were the most efficient catalysts compared to those comprising only the chelating ligands, likely as a result of the large open channels present due to the incorporation of less bulky secondary ligands.

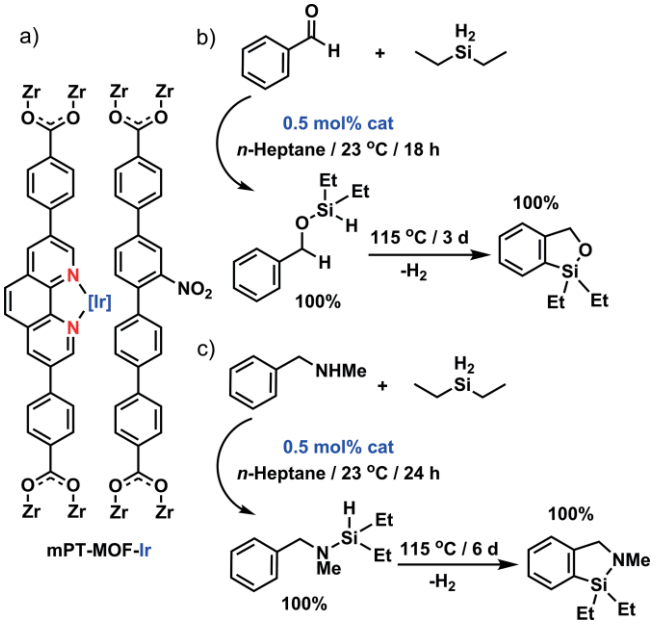

Figure 17. a) Schematic illustration of mPT-MOF-Ir highlighting both ligands incorporated in the MOF, alongside catalytic conditions investigated during the preparation of b) benzoxasiloles and c) azasilolanes.

Efficient Zr MOF based enantioselective heterogeneous catalysts have been synthesised by incorporating extended chiral BINAP [2,2′-bis(diphenylphosphanyl)-1,1′-binaphthyl] dicarboxylate ligands into UiO-type MOFs.[71] This so-called BINAP-MOF with general formula $[Zr_6O_4(OH)_4(Ligand)_6]_n$ (see part a of Figure 18 for the extended chiral BINAP based ligand) adopts the inherent chirality of the bridging ligands and crystallises in the *F*23 space group, with the extended ligands resulting in a highly porous structure with a solvent accessible void space of 76.3 %. Postsynthetic metalation was successfully demonstrated with either Rh [bis(norbornadiene)rhodium(I) tetrafluoroborate] or Ru [bis(2-methylallyl)(1,5-cyclooctadiene)ruthenium(II)], enabling a broad scope of catalytic activities to be achieved by judicious choice of the incorporated active metal. Rh-BINAP-MOF (that is the rhodium metalated BINAP-MOF) was observed to be an efficient catalyst for the conjugate addition of arylboronic acids to 2-cyclohexenone with enantiomeric excess values in excess of 99 %, whilst being 3 times more active than the homogeneous control. In contrast, Ru-BINAP-MOF (that is the ruthenium metalated BINAP-MOF) was found to be highly active for the hydrogenation of β-keto esters (Figure 18a) and substituted alkenes. A later study on Rh-BINAP-MOF showed that by using a mixed ligand strategy, where the second ligand does not contain metal binding sites and contains considerably less steric bulk, a catalytic framework with more open and accessible channels results.[72] The mixed ligand MOF was found to be an active catalyst for sterically demanding substrates when the conventional BINAP-MOF was no longer active.

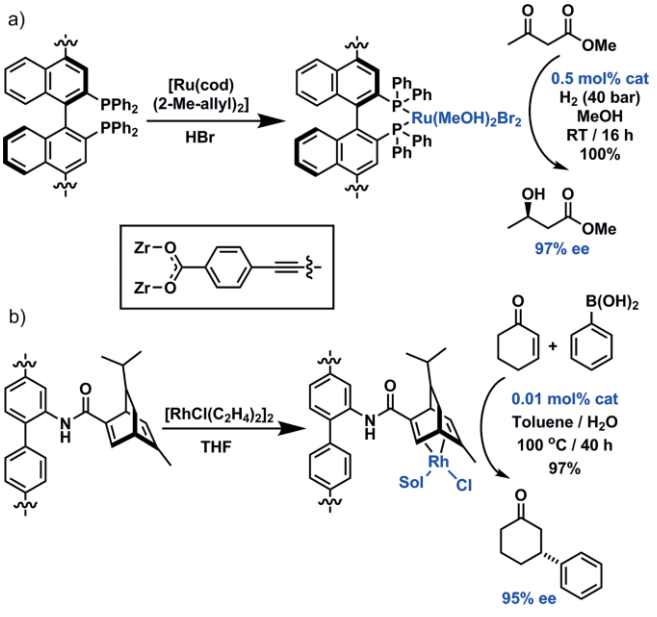

Figure 18. a) Schematic illustration of the chiral BINAP-MOF alongside the catalytic hydrogenation of β-keto esters that was studied for the Ru metalated species. b) Schematic illustration of the chiral MOF containing pendant chiral diene moieties (E_2-MOF) with the catalytic activity of the MOF for 1,4-additions of arylboronic acids to α,β-unsaturated ketones exemplified.

An alternative approach to obtain an enantioselective Zr MOF catalyst was to incorporate pendant chiral diene moieties.[73] The chiral diene containing UiO-type MOF, with general formula $[Zr_6O_4(OH)_4(Ligand)_6]_n$ (see part b of Figure 18 for the chiral diene based ligand), termed E_2-MOF, was proposed to be more efficient than the BINAP-MOF due to the decrease in steric demand, which should result in improved access of the reagents and consequently transport of the product from the active site. E_2-MOF was metalated with either $[RhCl(C_2H_4)_2]_2$ or $Rh(acac)(C_2H_4)_2$ and the resultant materials were investigated as heterogeneous catalysts for the asymmetric 1,4-addition of arylboronic acids to α,β-unsaturated ketones (Figure 18b) or asymmetric 1,2-addition of arylboronic acids to aldimines respectively. The potential of E_2-MOF•Rh(acac) is realised as better

yields and enantioselectivities were obtained when compared with the homogeneous control.

Considerable attention has been directed towards the metalation of free-base porphyrin containing Zr MOFs.[17b] Two Zr MOFs containing porphyrin units were synthesised using the tetratopic H_4-TCPP-H_2 [tetrakis(4-carboxyphenyl)porphyrin] ligand, with the traditional 12-connected $Zr_6O_4(OH)_4$ cluster observed in MOF-525 and an 8-connected $Zr_6O_8(H_2O)_8$ cluster observed in MOF-545, also described as PCN-222 (Figure 1d shows the solid-state structure of PCN-222-Fe).[17a] The resulting structures were highly porous with BET surface areas of 2620 $m^2 g^{-1}$ and 2260 $m^2 g^{-1}$ for MOF-525 and MOF-545, respectively, however the high porosity of the structures did not negatively impact their stability, with both MOFs observed to be stable in acidic and aqueous environments. Unlike other porphyrin containing MOFs, the porphyrin units are not metalated as Zr^{IV} ions are not coordinated during synthesis. The presence of both permanent porosity and free porphyrin sites enables opportunities for postsynthetic metalation, with MOF-525 able to be quantitatively metalated with iron chloride to form MOF-525-Fe. The benefits of postsynthetic metalation is realised as MOF-525-Fe could not be obtained by direct synthesis with the pre-metalated ligand (H_4-TCPP-FeCl).

Thin films of MOF-525 have been grown on conductive FTO (FTO = fluorine doped tin oxide) glass substrates and subsequently postsynthetically metalated with either cobalt or zinc, with metalation confirmed by UV/Vis spectroscopy on sodium hydroxide MOF digests.[74] Cyclic voltammetry was used to determine the electrochemical activity of the films and compared with free-base MOF-525. Co-MOF-525, containing Co^{III}, exhibited a much larger redox wave, suggesting that the materials electrochemical properties have been improved upon postsynthetic metalation. However, Zn-MOF-525 thin films demonstrated the greatest potential, with a large redox wave obtained at a lower potential (≈ 0.7 V vs. ≈ 0.8 V). Further chronoamperometric experiments were in close agreement with the electrochemical activity observed, with apparent diffusion coefficients (D_{app}) of the films decreasing in the order of Zn-MOF-525, then Co-MOF-525 and finally MOF-525. These results suggest that faster ion mobility or charge hopping is responsible for the increased electrochemical activity observed, highlighting that postsynthetic metalation is useful for improving materials properties.

An extended MOF-525 analogue, termed FJI-H6 and containing H_2TBPP {H_2TBPP = 4′,4‴,4⁗,4⁗⁗-(porphyrin-5,10,15,20-tetra-yl)tetrakis[(1,1′-biphenyl)-4-carboxylate]} ligands was reported, resulting in a highly porous structure containing 2.5 nm pores and a BET surface area of 5033 $m^2 g^{-1}$.[75] Access to single crystals of FJI-H6 unambiguously confirmed that postsynthetic metalation of the porphyrin units is possible, with a single-crystal to single-crystal transformation observed upon treatment with $Cu(NO_3)_2$ in DMF at 85 °C, resulting in FJI-H6(Cu) (Figure 19). The Cu^{II} ions occupy the square planar N_4 coordination site in the porphyrin units as expected, resulting in axial positions that are uncoordinated. Both FJI-H6 and FJI-H6(Cu) were investigated as catalysts for the cycloaddition of CO_2 with chloropropylene oxide to form the corresponding cyclic carbonate. Under the conditions examined, FJI-H6(Cu) outperformed the parent MOF by ca. 9 %, and interestingly retained its crystallinity, which was not the case for the parent MOF.

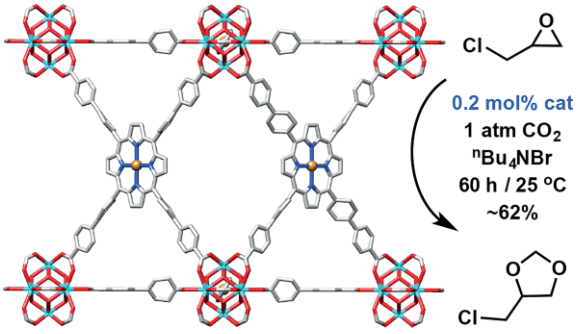

Figure 19. Representation of the crystal structure of FJI-H6(Cu), which is generated by postsynthetic metalation of the freebase porphyrin MOF (FJI-H6) and catalyses the cycloaddition of CO_2 and chloropropylene oxide. Redrawn from CCDC deposition 1043281.

Ligand design is crucial for the metalation of Zr MOFs; provided there are potential metal chelation sites these appear to undergo facile metalation, which is now evident from the many examples that have been reported. The hard properties of Zr^{IV} ions mean that they typically bind to the carboxylate functionalities used to construct the MOF, resulting in free metal chelation sites which can then be metalated with a number of substrates, many of which are introduced with specific catalytic applications in mind.

6. Postsynthetic Exchange

An alternative route for postsynthetic functionalisation of MOFs is to exchange framework constituents – either the ligands or the metals, and either completely or in a controlled manner – to provide access to functionalised materials not usually obtainable via direct synthesis.[7b] Several acronyms have been given to these processes with postsynthetic exchange (PSE)[7a] or solvent assisted linker exchange (SALE)[76] commonly employed, however, for simplicity we will refer to PSE to denote postsynthetic ligand exchange and transmetalation to indicate postsynthetic metal-ion exchange.

Postsynthetic exchange of Zr MOFs was reported in 2012 by Cohen et al., using aerosol time of flight mass spectrometry (ATOFMS) to detect exchange on individual particles.[77] Samples of UiO-66-Br and UiO-66-NH_2 were suspended in water for 5 days, with ATOFMS revealing that greater than 50 % of the MOF particles underwent exchange. The exchange process was found to be dependent on the solvent, with highest levels of exchange observed in water, followed by DMF, methanol and chloroform. An alternative exchange procedure was investigated, wherein UiO-66-Br was submersed in an aqueous solution containing NH_2-bdc, and it was found that 76 % of the Br-bdc ligands could be replaced by NH_2-bdc (Figure 20). Interestingly, the converse exchange of Br-bdc into UiO-66-NH_2 under similar conditions was found to occur to a much lesser degree, likely due to a number of different factors, which could reasonably include donor abilities, solubility and steric effects.

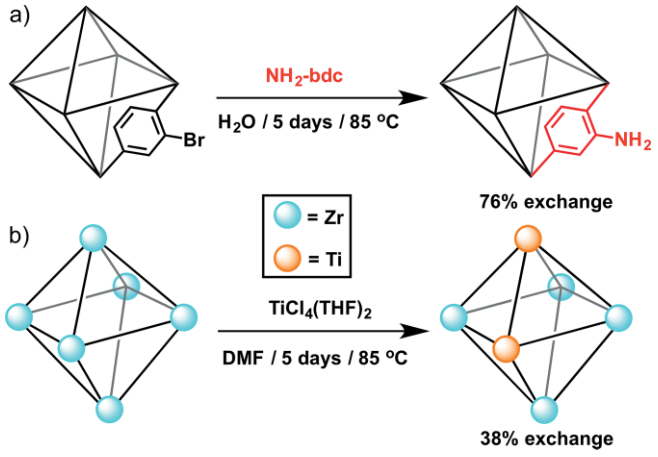

Figure 20. Postsynthetic exchange in UiO-66 series MOFs. a) Postsynthetic linker exchange of Br-bdc for NH_2-bdc in UiO-66-Br. b) Postsynthetic metal exchange of Zr for Ti in UiO-66.

During a later study, UiO-66 was postsynthetically exchanged with [FeFe](dcbdt)$(CO)_6$ (dcbdt = 1,4-dicarboxybenzene-2,3-dithiolate) (Figure 21a) resulting in substitution of 14 % of the bdc ligands for the thermally unstable [FeFe] complex.[78] The structural similarity of the [FeFe] subunit with [FeFe] hydrogenases prompted the examination of the material for photocatalytic hydrogen production, with the [FeFe] containing MOF found to be an efficient catalyst, outperforming the homogeneous reference system both in terms of reaction rate and hydrogen production (Figure 21b). This is due to the improved stability of the [FeFe] complex when contained within the MOF, whilst site localization also hinders charge recombination.

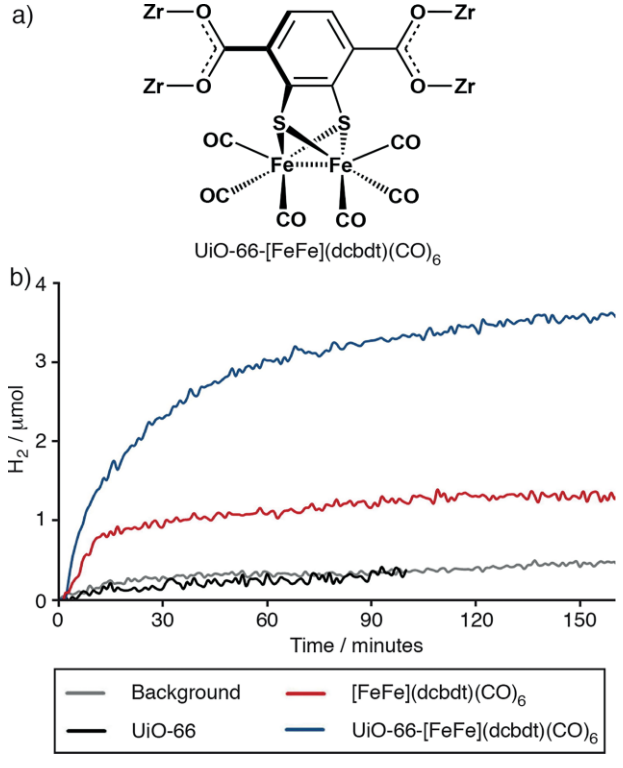

Figure 21. a) The [FeFe] hydrogenase mimic incorporated into UiO-66 by postsynthetic exchange. b) Comparison of photocatalytic H_2 evolution showing that UiO-66-[FeFe](dcbdt)$(CO)_6$ outperformed both the unfunctionalised MOF and the homogeneous catalytic system. Reproduced (modified) with permission from ref.[78] Copyright (2013) American Chemical Society.

Similarly, UiO-66 thin films grown on FTO substrates were postsynthetically exchanged with CAT-bdc (2,3-dihydroxy-1,4-benzenedicarboxylate), resulting in incorporation of chelating units (63 % CAT-bdc) that in turn could be postsynthetically metalated with aqueous $FeCl_3$ solutions in a two-step process.[79] PXRD and SEM indicated that crystallinity and particle morphology were retained, and with this general procedure established, attempts to incorporate [FeFe](dcbdt)$(CO)_6$ were investigated. PSE of the thin films resulted in higher levels of incorporation relative to the bulk samples (≈ 32–35 % vs. 14 %), likely due to the increased solid-liquid interphase. Fine control of the reagent concentrations resulted in films of varying thickness, which was observed to determine the electrochemical activity of the MOF films.

Microcrystalline UiO-66 samples synthesised using formic acid (100 equiv.) as a modulator revealed an unusually high surface area of 1730 $m^2\ g^{-1}$, while pore size distributions revealed the presence of a 3.9 nm mesopore.[80] The mesoporosity of UiO-66 prepared via this method was predicted to facilitate postsynthetic exchange of bdc ligands from the framework. The ligands btec (btec = 1,2,4,5-benzenetetracarboxylic acid) or ma (ma = benzenehexacarboxylic acid) were metalated with Li^+, Na^+ and K^+, resulting in six different salts, which were subsequently investigated for their exchange into UiO-66. The extent of ligand exchange varied, with the highest exchange ratios obtained for the Na salts. Of the MOFs obtained, UiO-66-$(COONa)_2$-ex (that is UiO-66 postsynthetically exchanged with sodium 1,2,4,5-benzenetetracarboxylate) demonstrated the greatest potential in CO_2 separation, with a CO_2/N_2 selectivity of 33.3, compared to 19.1 obtained for parent UiO-66. Alternatively, UiO-66 has been postsynthetically exchanged with flexible alkanedioic acids [$HO_2C(CH_2)_{n-2}CO_2H$] to result in a series of materials denoted as UiO-66-ADn, where n = 4, 6, 8 or 10.[81] In this example, PSE occurs in a 1:2 manner (one bdc ligand is replaced by two alkanedoic acid ligands) which results in pendant carboxyl moieties within the MOF cavities due to the mismatch of the ligand lengths. In the case of UiO-66-AD6, which contains adipic acid that is of a similar length to bdc, 1:1 exchange may also occur. The functionalised materials were subsequently investigated for their CO_2 adsorption capacities, with UiO-66-AD6 demonstrating increased capacities of 34 % and 58 % relative to parent UiO-66 at 298 K and 323 K respectively.

Postsynthetic exchange has also been performed on extended Zr MOFs, such as UiO-68-$(CH_3)_2$, containing 2′,5′-dimethyl-*p*-terphenyl-4,4′′-dicarboxylate ligands, where an iridium *N*-heterocyclic carbene (NHC) metallolinker was incorporated into the framework (Figure 22a).[82] Direct synthesis of the mixed ligand MOF was also considered, however, fine-tuning of the PSE conditions (methanolic ligand solution, 60 °C, 24 h) resulted in higher loadings of the metalloligand within the framework (17 % vs. 29 % as per ^1H NMR spectroscopic analysis). Isomerisation of 1-octen-3-ol to 3-octanone was investigated in the presence of the Ir-containing MOFs (obtained via

direct synthesis and PSE), however leaching of Ir was detected from the directly synthesised material, although this was not significant for the exchanged MOF. The Ir-containing exchanged UiO-68 type MOF proved to be an efficient catalyst, resulting in 99 % conversion without a loss of activity over three catalytic cycles (Figure 22b).

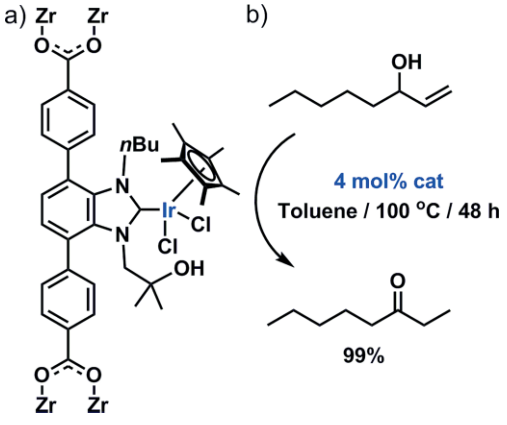

Figure 22. a) A terphenyl-dicarboxylate *N*-heterocyclic carbene linker which can be postsynthetically exchanged into UiO-68-$(CH_3)_2$, resulting in a MOF that can b) catalyse the isomerisation of 1-octen-3-ol to 3-octanone.

The accounts highlighted above prove the enormous potential of postsynthetic linker exchange in accessing specialised materials, many of which have demonstrated significant potential for catalytic applications utilising delicate active site functionality that would not normally survive direct synthetic methods. In addition to this incorporation of highly functionalised ligands, significant synthetic efforts have focused on the preparation of topologically analogous MOFs containing alternative metal ions. UiO-66 series MOFs constructed by hafnium,[83] uranium,[84] thorium[85] and cerium[86] are known, however there are no reported titanium UiO-type frameworks. As such, the incorporation of titanium has been investigated extensively via postsynthetic transmetalation, a route to the functionalisation of the secondary building units (SBUs) of Zr MOFs, enabling the insertion of alternative metal ions and resulting in mixed-metal MOFs which may offer improved characteristics specific to the new metal ions.

Incorporation of Ti^{IV} into UiO-66 was first reported in 2012 by Cohen et al., whereby as-synthesised UiO-66 was immersed in DMF solutions containing Ti^{IV} sources.[7a] Using $TiCl_4(THF)_2$ as the Ti^{IV} source, loadings as high as 37.9 mol-% Ti were obtained (93 % of particles showed exchange by ATOFMS) with crystallinity retained during the transformation (Figure 20b). N_2 adsorption isotherms revealed that porosity was also retained, suggesting that metal ion substitution had occurred and that Ti^{IV} ions were not located within the pores. Titanium-exchanged UiO-66 was later investigated as a catalyst for the oxidation of cyclohexene. Catalytic performance improved at 70 °C although this was still not as efficient as UiO-66 containing Ti^{IV} supported at the nodes (Ti^{IV} anchored onto the capping hydroxyl groups), due to the tetrahedral coordination environment of the Ti^{IV} supported material (in comparison to the 7- or eight-coordinate Ti^{IV} ions in the transmetalated species which is dependent upon the extent of framework hydroxylation), as revealed from XPS (X-ray photoelectron spectroscopy) analysis.[87]

Transmetalated UiO-66 samples containing Ti^{IV} were subsequently investigated for their ability to improve CO_2 uptake capacities.[88] UiO-66 samples containing Ti^{IV} loadings as high as 56 mol-% were obtained [denoted UiO-66(Ti_{56})] by allowing the transmetalation process to occur over a longer period of time. The CO_2 uptake capacity at 273 K was observed to increase from 2.2 mmol g^{-1} for UiO-66 to 4 mmol g^{-1} for UiO-66(Ti_{56}), representing an enhancement of 81 %. The authors suggest that the decrease in the octahedral pore diameter upon substitution with Ti^{IV} results in an increased isosteric heat of adsorption (Q_{st}) for CO_2 (Figure 23a) and this coupled with the decreased density of the framework is responsible for the increased uptake. This methodology was investigated for exchanging Ti^{IV} into UiO-66 mixed matrix membranes, with the resulting membranes demonstrating dramatically improved permeabilities for CO_2 compared to parent UiO-66 membranes (as high as 153 % improvement) without affecting selectivity.[89]

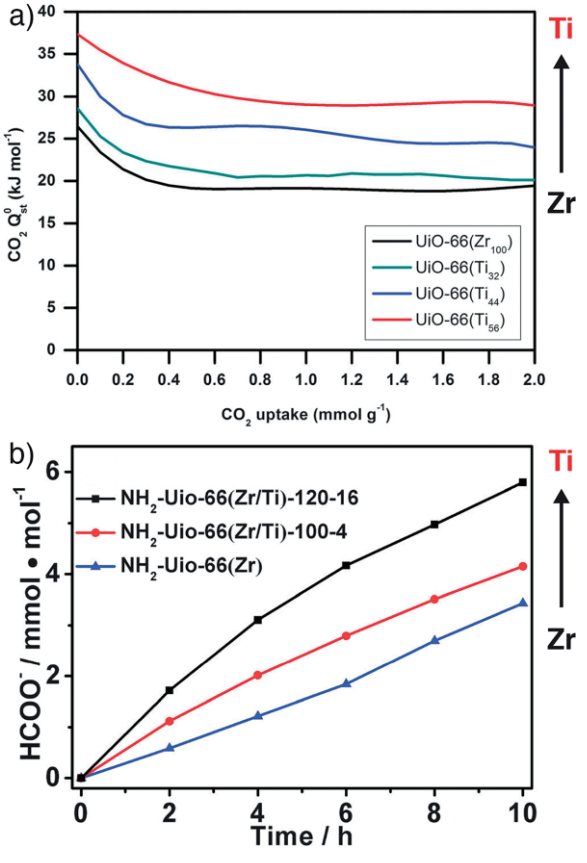

Figure 23. a) Increasing isosteric heats of adsorption for CO_2 in UiO-66 as more Zr is exchanged for Ti. Reproduced (modified) with permission from ref.[88] Copyright (2013) Royal Society of Chemistry. b) Photocatalytic reduction of CO_2 to formate by UiO-66-NH_2 is also enhanced by exchange of Zr for Ti. The samples NH_2-UiO-66(Zr/Ti)-100-4 and NH_2-UiO-66(Zr/Ti)-120-16 have 34 % and 57 % of Zr cations exchanged for Ti, respectively. Reproduced (modified) with permission from ref.[90] Copyright (2015) Royal Society of Chemistry.

Following the interest surrounding improving CO_2 uptake capacities, Ti-doped UiO-type MOFs have been investigated for photocatalytic CO_2 reduction.[90] Transmetalation of UiO-66-NH_2

in DMF solutions containing $TiCl_4(THF)_2$ at different incubation temperatures and durations revealed that up to 57 mol-% Ti^{IV} could be incorporated [120 °C, 16 d, denoted as NH_2-UiO-66(Zr/Ti)-120-16 in Figure 23b]. Photocatalytic reduction of CO_2 to formate was investigated using both pristine UiO-66-NH_2 and transmetalated materials. Under the conditions investigated, 57 % Ti-exchanged UiO-66-NH_2 resulted in the production of 1.7 times more formate than parent UiO-66-NH_2. The improved performance were rationalised by a combination of low temperature electron spin resonance experiments and DFT calculations, which suggest that incorporation of Ti^{IV} into the cluster facilitates the transfer of electrons from the NH_2-bdc ligands upon photo-excitation to the metal ion cluster. The reduced Ti^{III} is then able to act as an electron donor as the Zr^{IV} is reduced to Zr^{III}, resulting in improved electron transfer and ultimately improved catalytic abilities. A similar study extended the range of transmetalated UiO-type MOFs containing Ti^{IV}, to a UiO-66 analogue containing mixed ligands.[91] Mixed ligand UiO-66-NH_2, containing NH_2-bdc as well as 2,5-diamino-1,4-benzenedicarboxylate (14 %) was transmetalated, resulting in a material with hexametallic nodes of average formula $\approx Zr_{4.3}Ti_{1.7}$. The mixed ligand MOF was also investigated for the photocatalytic reduction of CO_2, alongside Ti substituted UiO-66-NH_2, and it was realised that the mixed ligand MOF was a more superior catalyst due to the introduction of new energy bands which facilitate improved light absorption and charge transfer.

While exchange of either bridging ligands or the metal ions of Zr MOFs has proven useful for a number of applications, the specific inclusion of either secondary metals or organic species at the Zr_6 clusters has also been highlighted as an important route to access functionalised materials. In this context secondary species are incorporated into the framework without the necessary exchange of parent framework constituents, so intentionally defective UiO-66 series MOFs (exposed cluster sites are present due to the missing linkers) or MOFs containing lower connected Zr_6 clusters have been targeted as their clusters can be accessed and subject to a suite of potential modifications.

7. Postsynthetic Cluster Modification

Coordination modulation[49] – the deliberate addition of foreign molecules to synthetic mixtures – is routinely employed to improve the crystallinity of, and in extreme cases enable access to otherwise unobtainable Zr MOFs.[92] The modulating agent alters the crystallisation kinetics,[93] presumably by competing with the bridging ligands for coordination to the Zr_6 cluster or by pre-forming $Zr_6O_4(OH)_4(CO_2\text{-}R)$ building blocks.[94] In addition to improved synthetic reliability, coordination modulation has also resulted in the promotion of defects (typically in the form of missing linkers and cluster incorporated monodentate modulators),[95] which are prevalent in Zr MOFs and have recently been structurally characterised in UiO-66 on the molecular level using single-crystal X-ray diffraction.[96] A variety of modulating agents have been investigated, including but not limited to, hydrochloric acid,[95b] formic acid,[96] hydrofluoric acid,[97] trifluoroacetic acid[98] and recently amino acids.[99] During Zr MOF syntheses it is difficult to predict whether the modulator will be incorporated within the final structure,[95a,98] and if so how the properties of the material will be affected.[10f,95d,100] Defective Zr MOFs represent an attractive route to obtain materials with unprecedented reactivity, although an understanding of their true potential is yet to be realised as this area still remains relatively unexplored.

An interesting study conducted by Vos et al. reported the synthesis of UiO-66 using a combination of hydrochloric (HCl) and trifluoroacetic acid (TFA), resulting in highly crystalline materials that were subsequently investigated as catalysts for the "ene"-type cyclisation of citronellal to isopulegol (Figure 24a).[98]

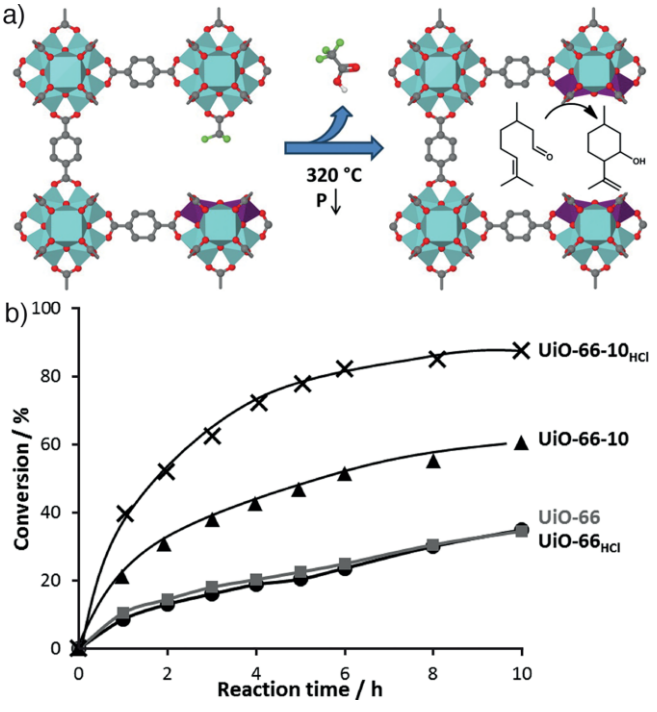

Figure 24. a) Schematic showing thermal removal of TFA from defects in UiO-66 to create a Lewis acid catalyst for citronellal cyclisation. b) Comparison of conversion vs. time for different samples, with the most defective MOF being the most catalytic. Reproduced (modified) with permission from ref.[98] Copyright (2013) American Chemical Society.

UiO-66-10_{HCl}, that is UiO-66 synthesised in the presence of 10 equiv. of TFA and 1 equiv. of HCl, was observed to contain both physisorbed and cluster bound TFA (trifluoroacetate had partially replaced bdc) from thermal analysis and ^{19}F solid-state NMR spectroscopy. Thermal treatment of UiO-66-10_{HCl} was followed by in-situ IR spectroscopy, revealing that dehydroxylation of the Zr cluster begins prior to removal of trifluoroacetate, although the two processes occur simultaneously at higher temperatures. Postsynthetic thermal treatment results in $Zr_6O_8(bdc)_4$ – a highly defective material containing Zr_6 clusters surrounded by 8 carboxylates rather than the usual 12 – which has a high number of Lewis acid (Zr^{IV}) sites and increased pore dimensions, resulting in dramatically improved catalytic performances. UiO-66-10_{HCl} is considerably more active in the cyclisation of citronellal to isopulegol (Figure 24b), while in the

Meerwein reduction of 4-*tert*-butylcyclohexanone with 2-propanol, conversions of 7 % vs. 93 % are achieved for UiO-66-NO_2 and UiO-66-NO_2-10_{HCl}, respectively.

Furthermore, the dynamic nature of the Zr-modulator bond can be exploited to result in postsynthetic substitution of the cluster bound modulators, either for alternative modulators or for the bridging ligand, effectively "repairing" defect sites. Applying this defect repair strategy to UiO-67 crystals synthesised using benzoic acid and containing appreciable amounts of defects, gave crystals of sufficient quality for single-crystal X-ray diffraction.[95a] Substitution of the modulator was also observed with proline, which may result in chiral materials, while incorporation of chromium into defective UiO-66 and UiO-67 samples (presumably at defect sites) resulted in catalytic materials for acetaldehyde trimerisation.

An alternative "repair" strategy has been applied to single crystals of PCN-700, resulting in the first Zr MOF bearing ligands that not only present different chemical functionality but are also of different lengths, resulting in what are commonly known as multivariate MOFs.[101] The staggered arrangement of the phenyl rings in the 2,2′-dimethylbiphenyl-4,4′-dicarboxylate ligands of PCN-700 results in a **bcu** topology containing 8 connected nodes (Figure 25a), in contrast to the 12 connected nodes of the UiO-66 series with **fcu** topology. The structure contains two "pockets" of different lengths (7.0 and 16.4 Å) which can accommodate linear dicarboxylate ligands, and as such the authors examined the postsynthetic installation of bdc (Figure 25b) and tpdc-Me_2 (tpdc-Me_2 = 2′,5′-dimethyl-*p*-terphenyl-4,4′′-dicarboxylate, Figure 25c). The postsynthetic order of addition of the bridging ligands is important, as upon insertion of the first ligand the size of the second pocket is altered (Figure 25d), although by careful considerations a multivariate MOF containing 3 ligands was isolated and unambiguously characterised using single-crystal X-ray diffraction, whilst functionalised ligands such as NH_2-bdc can also be incorporated, highlighting the versatility of this technique.

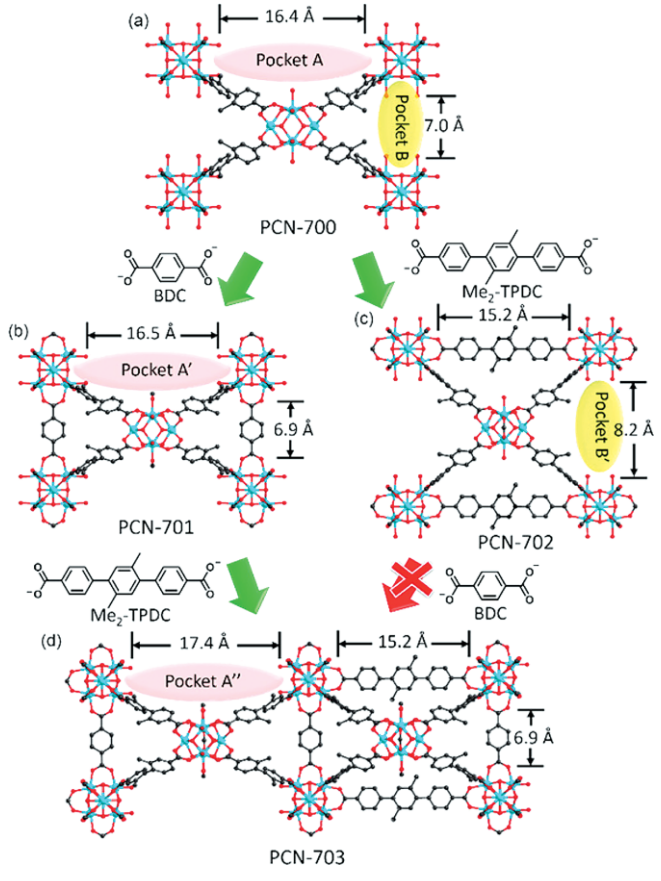

Figure 25. Crystal structures of a) PCN-700, which contains vacancies, or "pockets" between 8-connected nodes that can be filled by postsynthetic addition of 1,4-benzenedicarboxylate, to give b) PCN-701, and 2′,5′-dimethyl-terphenyl-4,4′′-dicarboxylate, to give c) PCN-702. Both pockets can be filled to give d) PCN-703, but only if the smaller pocket is occupied by 1,4-benzenedicarboxylate first. Reproduced with permission from ref.[101] Copyright (2015) American Chemical Society.

The presence of either μ_3-OH or terminal OH or H_2O moieties at Zr nodes, whose concentration depends on both the defect concentration and topology of the MOF, results in a range of possible sites for functionalisation of the Zr_6 clusters, and the Brønsted acidity of these groups has been calculated for a range of Zr MOFs using potentiometric titrations.[102] Alternatively, defect sites within Zr MOFs present attachment sites for secondary ligands that contain potential coordinating sites, such as carboxylates or phosphonates. For example, defect-free and intentionally defective UiO-66 were synthesised, and then exposed to DMF solutions containing oxalic acid at room temperature for 2 hours.[103] Oxalic acid was successfully incorporated into defective UiO-66 (Figure 26a) however, no incorpora-

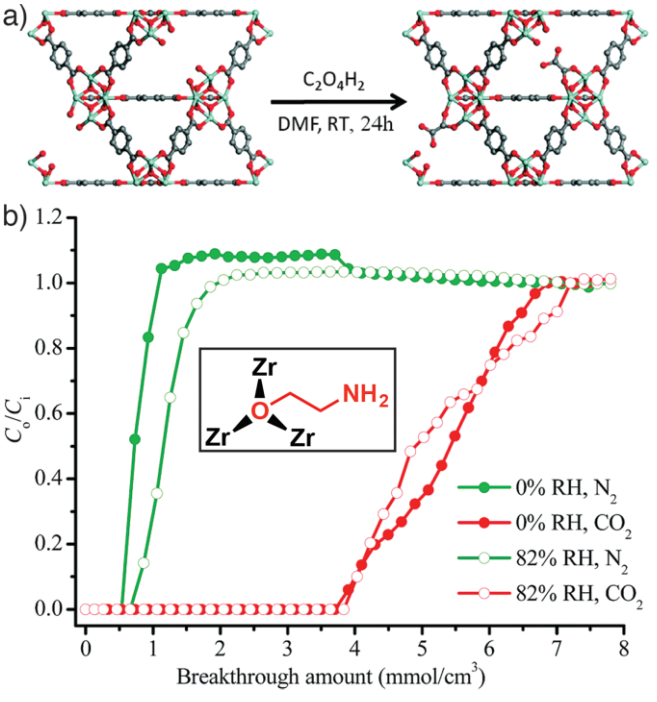

Figure 26. a) Schematic illustration of the PSE of oxalic acid into UiO-66, highlighting covalent attachment to the Zr_6 node at defect sites. Reproduced (modified) with permission from ref.[103] Copyright (2015) Centre National de la Recherche Scientifique (CNRS) and The Royal Society of Chemistry. b) UiO-66-ea breakthrough curves for 10:90 CO_2/N_2 (*v*/*v*) mixtures at 313 K and 1 atm with capacities at 0 % and 82 % relative humidity shown. C_o and C_i are the concentrations of each gas at the outlet and inlet respectively. Reproduced (modified) with permission from ref.[104] Copyright (2015) Royal Society of Chemistry.

tion was observed for the defect-free material, and hence post-synthetic linker exchange can be excluded as a method of incorporation. During breakthrough experiments with a number of toxic compounds, UiO-66-ox (UiO-66 containing cluster bound oxalic acid) greatly outperformed both the defective and defect-free UiO-66 samples in terms of storage capacities for SO_2 and NO_2, whilst only a modest improvement was observed for NH_3.

An alternative strategy was employed for the installation of ethanolamine onto the Zr_6 clusters of UiO-66, by exposing dehydrated UiO-66 (UiO-66 heated at 300 °C for 1 hour under an N_2 atmosphere) to an anhydrous toluene solution containing ethanolamine (ea).[104] Similar to UiO-66-ox, UiO-66-ea $[Zr_6O_4(OH)_2(ea)_2(bdc)_6]_n$ contains pendant amino moieties (ethanolamine is grafted onto Zr_6 clusters at the triangular windows formed between three Zr^{IV} ions, partially replacing bridging μ_3-OH moieties) which were expected to improve the material's CO_2 adsorption capacity. Breakthrough experiments under simulated flue gas conditions (10:90 CO_2/N_2, 313 K) revealed that the purification capacity of UiO-66-ea is ca. 18 times that of non-modified UiO-66, and interestingly this capacity is maintained even under 82 % relative humidity (Figure 26b).

The availability of terminal OH and H_2O ligands on the Zr_6 clusters of NU-1000 $\{[Zr_6(\mu_3\text{-}O)_4(\mu_3\text{-}OH)_4(OH)_4(OH_2)_4(TBAPy)_2]_n$, where TBAPy = 1,3,6,8-tetrakis(*p*-benzoate)pyrene} to undergo postsynthetic exchange has resulted in extensive research where this phenomenon has been exploited in a process the authors call SALI (Solvent Assisted Ligand Incorporation). In 2013, Farha et al. reported the incorporation of a series of perfluorinated alkanes of varying length onto the nodes of NU-1000.[105] Microcrystalline samples of NU-1000 were placed in contact with DMF solutions containing the desired perfluorinated aliphatic carboxylic acid and left to react at 60 °C for 18–24 hours (Figure 27a). The maximum uptake of the perfluorinated alkane ligands per Zr_6 node is 4, which would result in coordinatively saturated $Zr_6(\mu_3\text{-}O)_4(\mu_3\text{-}OH)_4(RCO_2)_{12}$ clusters, similar to those found in UiO-type MOFs. The resultant materials, SALI-*n*, where *n* corresponds to the length of the perfluorinated alkane chain, could be obtained in quantitative yields for the lower alkane species, which dropped slightly as the chain length increased presumably due to steric effects. CO_2 adsorption experiments revealed that, despite the additional functionality occupying pore volume, CO_2 uptake capacities increased across the SALI-*n* series, with the Q_{st}^0 value for SALI-9 being twice that of unmodified NU-1000 (Figure 27b). It was later found that NU-1000 materials containing perfluorinated alkanes (obtained via SALI) demonstrate enhanced water stabilities. The node functionalisation removes the polar terminal OH and H_2O ligands, which interact strongly with water, while the incorporated fluorinated ligands prevent water from accessing the Zr_6 clusters.[106] Perfluorinated NU-1000 materials were subsequently loaded with Pd nanoparticles (confined within the pores), and investigated as catalysts for the C–H arylation of indoles in H_2O.[107]

An alternative strategy to improve the CO_2 capacity of NU-1000 was to incorporate "complementary organic motifs" (predesigned organic molecules that are complementary to the CO_2 quadrupole) at the Zr_6 nodes by SALI.[108] The complementary organic motifs were based upon either a 2,6-diacetylaminopyridine or an FMoc (FMoc = *N*-α-fluorenylmethyloxycarbonyl) protected triglycine peptide. The SALI products demonstrate similar volumetric uptakes with that of parent NU-1000, however the favourable CO_2 binding sites increase CO_2 uptake at low pressures, with Q_{st}^0 values increasing from ca. 17 kJ mol^{-1} (parent NU-1000) to ca. 27–28 kJ mol^{-1} (SALI products) to reflect this.

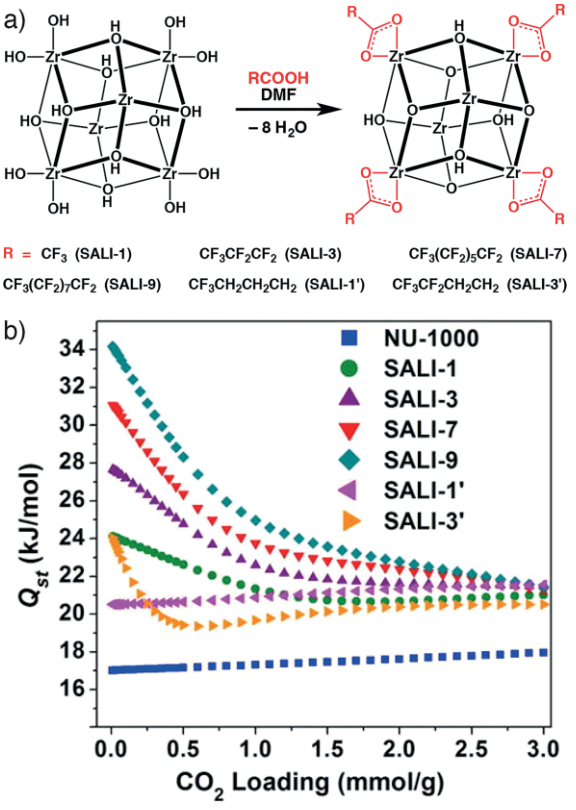

Figure 27. a) Schematic of Solvent Assisted Linker Incorporation (SALI) at the 8-connected node of NU-1000 to give fluorinated MOFs which b) offer improved isosteric heats of adsorption for CO_2. Reproduced (modified) with permission from ref.[105] Copyright (2013) American Chemical Society.

The scope of carboxylate containing compounds incorporated into NU-1000 via SALI was extended to include those containing pendant reactive handles, and thus further postsynthetic modifications such as the CuAAC "click" reaction and imine formation were performed.[109] SALI has also been performed on NU-1000 to incorporate either ferrocene[110] or tris-radical rotaxanes[111] for electrochemical applications. In the case of the ferrocene containing NU-1000 samples,[110] the ferrocene molecules (1 per Zr_6 node) are electrochemically addressable, implying that the activity comes from charge hopping between anchored ferrocene/ferrocenium (Fc/Fc^+) moieties. The presence of charge hopping mechanisms points towards potential for use in photoelectrochemical or electrocatalytic systems.

A halochromic NU-1000 derivative was obtained by performing SALI to incorporate carboxylnaphthofluorescein (CNF) within the framework, and although low loadings were ob-

tained (0.12 molecules of CNF per Zr_6 node; the theoretical maximum is 4) the materials visibly changed colour when exposed to either acidic or basic solutions or vapours.[112] The SALI concept has been extended to enable the incorporation of ligands bearing terminal phosphonates into NU-1000, and the higher affinity of Zr^{IV} for phosphonates than carboxylates means that the pH range available for retention of the incorporated ligands is extended.[113] The ability of phosphonates to interact with the Zr_6 clusters has prompted investigations into their ability to degrade nerve agent simulants;[114] it has been realised that lower connected Zr clusters are more efficient,[115] resulting in improved hydrolysis rates and turnover frequencies. The CNF functionalised NU-1000 is an active catalyst for the degradation of nerve agent simulants, and with the acidic by-products changing the colour of the MOF, it thereby acts as a visual reporter for the presence of the nerve agent.[112] Treatment of NU-1000 with a phosphonic acid ligand containing bipyridine moieties [(2,2′-bipyridine-4-ylmethyl)phosphonic acid monohydrochloride] resulted in successful incorporation of the ligand, which upon treatment with trimethylamine presents free base pyridine sites which can be accessed and subsequently metalated.[116] Treatment with methanolic solutions of $NiCl_2$ results in the metalated MOF which contains ca. 1.5 Ni^{II} ions per Zr_6 node and is a highly active catalyst for ethylene dimerization.

Metalation of isolated $Zr_6O_4(OH)_4(RCOO)_{12}$ clusters has been studied,[117] hence it is no surprise that efforts have investigated this route for the incorporation of secondary metals into Zr MOFs. Reaction of UiO-67 powder with an ether solution containing [$AuMe(PMe_3)$] releases methane when the gold complex is successfully grafted onto the Zr-cluster (Figure 28a), allowing the extent of postsynthetic modification to be quantitatively

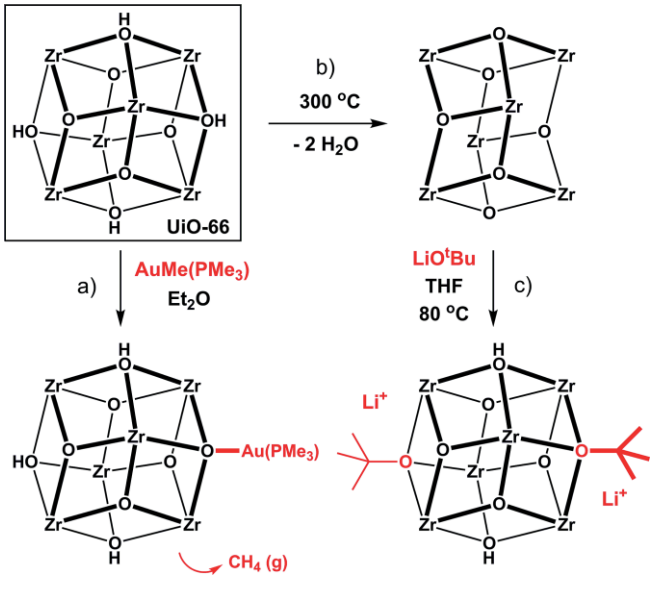

Figure 28. a) Schematic illustration for grafting of $AuMe(PMe_3)$ onto the nodes of UiO-66, with the associated release of methane. b) Dehydration of the $[Zr_6(\mu_3\text{-}O)_4(\mu_3\text{-}OH)_4]$ clusters of UiO-66, forming $[Zr_6O_6]$ clusters which are found to c) contain bound *tert*-butoxide anions upon treatment with lithium *tert*-butoxide.

measured. Spectroscopic techniques and elemental analysis were also used, providing evidence that $[Zr_6O_4(OH)_3(OAuPMe_3)(bpdc)_6]$ was obtained.[118] Under different reaction conditions, Long and co-workers successfully grafted lithium *tert*-butoxide onto the clusters of UiO-66 by first dehydrating the framework to form Zr_6O_6 clusters (Figure 28b).[119] Upon interaction with lithium *tert*-butoxide, which is expected to replace the now vacant μ_3-OH sites by a similar binding motif, 25 % of the available sites were found to be occupied by *tert*-butoxide anions (Figure 28c). Ionic conductivity measurements revealed that the lithium *tert*-butoxide grafted material behaves as a solid Li^+ electrolyte with a conductivity of 1.8×10^{-5} S cm^{-1} at 293 K.

This lithiation technique was also used in a later study, where a range of UiO-66 materials were investigated as self-detoxifying adsorbents of chemical warfare agents.[120] Defect free, lithium alkoxide grafted (prepared as described above), defective (containing cluster bound acetate) and acidic (containing cluster bound sulfate) UiO-66 were investigated, however the lithium alkoxide grafted material displayed the greatest hydrolytic activity, resulting in the efficient detoxification of chemical warfare agents containing hydrolysable P–F, P–O and C–Cl bonds.

Grafting of secondary metal ions onto the Zr_6 clusters of UiO-type MOFs has been highlighted as a potential route to obtain catalytic materials. Metalation of the cluster bound OH ligands (at missing linker defect sites) of UiO-66 with V^V upon reaction with a methanolic solution containing $VO(acac)_2$ (acac = acetylacetonate) at 50 °C, results in an active catalyst, even at temperatures as high as 350 °C, for the gas phase oxidative dehydrogenation of cyclohexene.[121] Alternatively, Ir functionalisation of Zr_6 nodes in UiO-66 was investigated, revealing that there are two possible sites for attachment of the Ir complexes, with only one site metalated at low Ir concentrations (MOF powder in contact with *n*-pentane solution containing Ir source).[122] The two different Ir sites present different reactivities; the Ir is more electropositive in one site than another, as revealed during catalytic ethylene hydrogenation studies.

Definitive evidence of the metalation process has been revealed by single-crystal X-ray diffraction, which has been used to provide snapshots at set time intervals (2, 4, 6, 12, and 24 h) of the metalation of single crystals of an 8-connected Zr MOF, linked by 2,2′-dimethylbiphenyl-4,4′-dicarboxylate ligands (PCN-700), with either Ni or Co.[123] The metal source (Co^{II} or Ni^{II}) was introduced as a DMF solution to single crystals of PCN-700 at 85 °C for 48 h, and it was observed that cluster metalation is accompanied by ligand migration, whereby the ligand dissociates from the Zr ion and attaches to the postsynthetically introduced metal ion. Overall, during metalation the 8-connected $[Zr_6O_4(OH)_8(H_2O)_4]$ cluster (Figure 29a) transforms to become a bimetallic $[Zr_6M_4O_8(OH)_8(H_2O)_8]$ (M = Co or Ni, Figure 29b) cluster, whilst maintaining crystallinity. The flexibility of the material is key, as the ligands are required to withstand torsional angle changes (13.2°), ultimately enabling the postsynthetic ligand migration and metalation to occur and crystallographic snapshots of the process to be collected (Figure 29c).

Gas phase metalation has emerged as an alternative method for the functionalisation of NU-1000, again taking advantage of

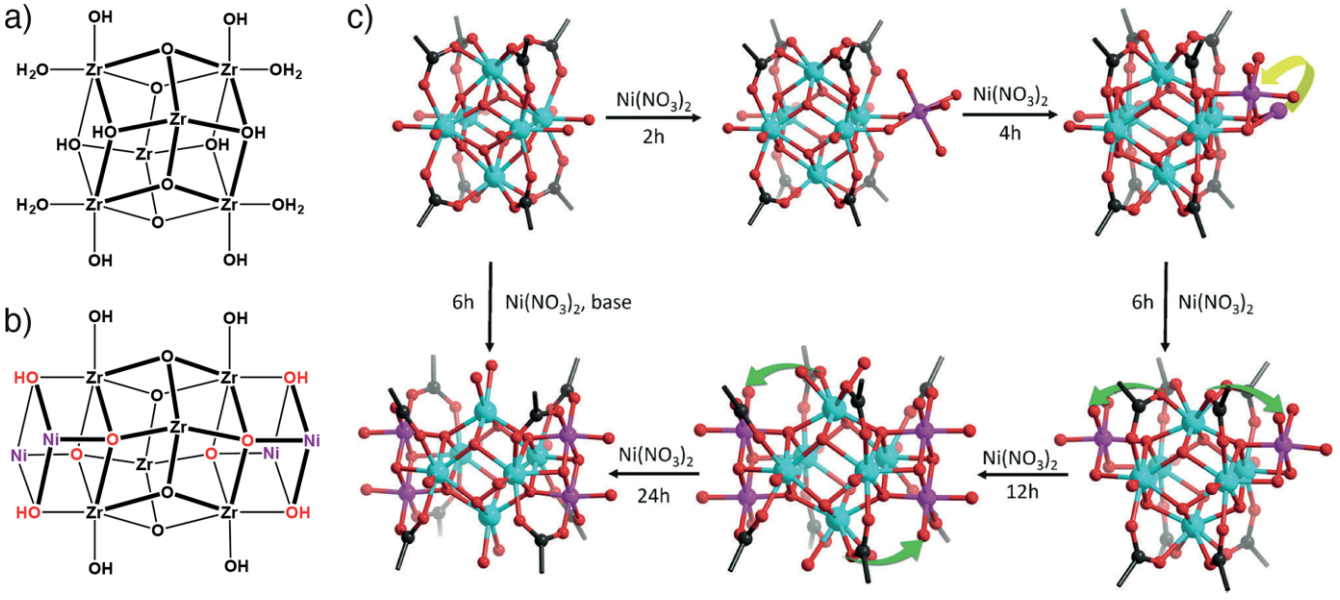

Figure 29. a) The 8-connected $Zr_6O_4(OH)_8(H_2O)_4$ cluster of PCN-700 and b) the bimetallic $[Zr_6Ni_4O_8(OH)_8(H_2O)_8]$ cluster that is formed upon metalation (terminal water ligands on Ni cations not shown for clarity). c) Crystallographic snapshots of the incorporation and migration of Ni cations at the cluster of PCN-700. Reproduced with permission from ref.[123] Copyright (2015) Wiley-VCH.

the terminal OH and H_2O ligands at its 8-connected clusters (Figure 30a), and has been termed Atomic Layer Deposition (ALD) in MOFs, shortened to AIM (Figure 30b).[18] Microcrystalline samples of NU-1000 were placed in an ALD reactor and exposed to $Zn(Et)_2$ or $Al(Me)_3$ at 140 °C or 120 °C respectively. ICP-OES revealed that metalation of NU-1000 was successful, suggesting that 0.5 Zn or 1.4 Al atoms were incorporated per Zr atom using very short experiment times (minutes), whilst only slightly better metalation yields were obtained for the corresponding liquid phase reactions performed over several hours.

DRIFTS (Diffuse Reflectance Infrared Fourier Transform Spectroscopy) was used to confirm that metalation occurred by reaction of the secondary metal atoms with the terminal OH groups. NU-1000-Zn, formed by AIM of NU-1000, was later synthesised and found to contain 4 Zn atoms per Zr_6 node, whilst DFT (density functional theory) calculations were used to precisely predict the location of the Zn atoms at the Zr_6 cluster. NU-1000-Zn was then transmetalated, allowing the Zn atoms to be post-synthetically exchanged (with varying successes observed) for Cu, Co and Ni which were unable to be prepared directly from solution phase reactions.[124]

This methodology was extended to include the metalation of NU-1000 thin films grown on FTO; Co installation was successful, resulting in 4.3 Co atoms per Zr_6 cluster, whilst EDS (Energy Dispersive X-ray Spectroscopy) was used to confirm that the thin film was uniformly metalated.[125] Electrochemical studies investigating the catalytic activity of the NU-1000-Co thin film for water oxidation revealed that the material is only marginally active at pH 10 or below, however at pH 11 the material is highly active, resulting in the formation of O_2 from OH^-, however, unfortunately at pH 11 the thin film degrades. AIM of bulk samples of NU-1000 was reported with Al and In

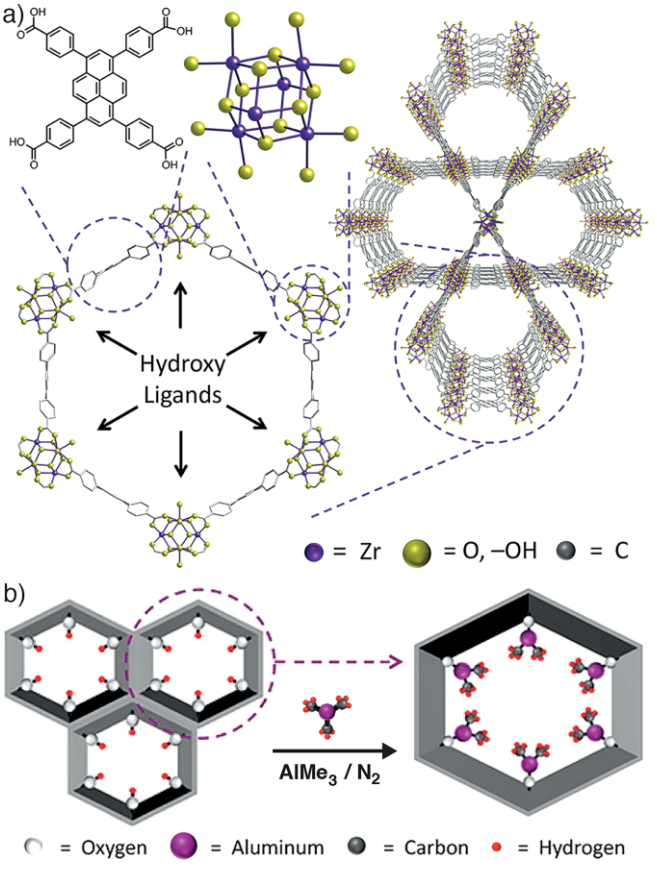

Figure 30. a) The solid state packing structure of NU-1000 is shown (right) and broken down to show both the TBAPy ligands and the Zr_6 clusters. Their connectivity is shown, highlighting the presence of pore directed terminal OH ligands. b) Schematic illustration of AIM of NU-1000 with $AlMe_3$ through reaction with the terminal OH ligands. Reproduced (modified) with permission from ref.[18] Copyright (2013) American Chemical Society.

by reacting the MOF with the trimethyl metal precursors.[126] The reaction between NU-1000 and $In(Me)_3$ is self-limiting and forms the predicted structure (two In atoms on each of the four faces of the Zr_6 node), whilst the more reactive Al precursor is not self-limiting and reacts with the framework, resulting in partial loss of crystallinity, highlighting that AIM conditions must be judiciously chosen for each MOF/metal system. Furthermore, NU-1000 has also undergone AIM with Co-S[127] or Ni[128] to result in catalytically active materials. The resulting NU-1000-Ni material was found to be an efficient catalyst for the oligomerisation of ethylene, which has important implications for the production of fuels and lubricants.

It has become apparent that vast opportunities exist for the modification of inorganic Zr_6 clusters within Zr MOFs, resulting in specialised materials, which have been investigated for gas storage/capture, catalysis and electrochemical applications. We anticipate that this area of research has the potential to be greatly expanded, as both concepts of defects and cluster modifications may be considered simultaneously, resulting in materials containing only slight structural/chemical modifications from their parent structures, yet the reactivity they present may be exceptionally different.

8. Conclusions and Outlook

In this microreview we have highlighted prominent examples of postsynthetic modifications that have been performed exclusively on metal-organic frameworks containing Zr^{IV} ions. The large number of articles discussed within, and the even greater number of articles on Zr MOFs that appear in the literature, highlight the extensive efforts that are currently being focused on Zr MOFs, which stems in part from their high chemical and mechanical stabilities and thus their ease of manipulation that renders them ideal platforms for functionalisation by postsynthetic modification to access materials not achievable by direct synthetic techniques. Frequently, early accounts of PSM focused on UiO-type MOFs containing $Zr_6O_4(OH)_4$ clusters, however lower connected structures, such as NU-1000, containing Zr_6-$(\mu_3\text{-}O)_4(\mu_3\text{-}OH)_4(OH)_4(H_2O)_4$ clusters, are now known and have received particular attention due to the availability of their terminal OH and H_2O ligands to undergo chemical modifications with a variety of substrates. The wide variety of modifications which have been successfully performed on Zr MOFs – covalent modifications (both pendant and integral), surface modification, metalation, linker exchange, metal exchange and modification of the inorganic cluster – highlight the potential to generate diverse structures with functionality suited to applications such as catalysis, selective adsorption and ionic conductivity. Through a combination of both the search for alternative modifications as well as new Zr MOFs with improved properties, PSM will ultimately play a key role in accessing next-generation materials. We also anticipate that much of the work that has been performed on Zr MOFs will be considered on analogous Hf MOFs which are topologically very similar but have been studied to a lesser extent.

Acknowledgments

The authors thank the Engineering and Physical Sciences Research Council (EPSRC) for support (EP/L004461/1). R. S. F. thanks the Royal Society for receipt of a University Research Fellowship.

Keywords: Metal-organic frameworks · Microporous materials · Zirconium · Postsynthetic modification

[1] a) J. R. Long, O. M. Yaghi, *Chem. Soc. Rev.* **2009**, *38*, 1213–1214; b) H.-C. Zhou, J. R. Long, O. M. Yaghi, *Chem. Rev.* **2012**, *112*, 673–674; c) H. Furukawa, K. E. Cordova, M. O'Keeffe, O. M. Yaghi, *Science* **2013**, *341*, 6149.
[2] a) J. L. C. Rowsell, O. M. Yaghi, *Angew. Chem. Int. Ed.* **2005**, *44*, 4670–4679; *Angew. Chem.* **2005**, *117*, 4748; b) K. Sumida, D. L. Rogow, J. A. Mason, T. M. McDonald, E. D. Bloch, Z. R. Herm, T.-H. Bae, J. R. Long, *Chem. Rev.* **2012**, *112*, 724–781; c) S. Ma, H.-C. Zhou, *Chem. Commun.* **2010**, *46*, 44–53.
[3] a) J. Lee, O. K. Farha, J. Roberts, K. A. Scheidt, S. T. Nguyen, J. T. Hupp, *Chem. Soc. Rev.* **2009**, *38*, 1450–1459; b) M. Yoon, R. Srirambalaji, K. Kim, *Chem. Rev.* **2012**, *112*, 1196–1231.
[4] a) C. Orellana-Tavra, E. F. Baxter, T. Tian, T. D. Bennett, N. K. H. Slater, A. K. Cheetham, D. Fairen-Jimenez, *Chem. Commun.* **2015**, *51*, 13878–13881; b) J. Della Rocca, D. Liu, W. Lin, *Acc. Chem. Res.* **2011**, *44*, 957–968; c) P. Horcajada, C. Serre, G. Maurin, N. A. Ramsahye, F. Balas, M. Vallet-Regí, M. Sebban, F. Taulelle, G. Férey, *J. Am. Chem. Soc.* **2008**, *130*, 6774–6780; d) A. C. McKinlay, R. E. Morris, P. Horcajada, G. Férey, R. Gref, P. Couvreur, C. Serre, *Angew. Chem. Int. Ed.* **2010**, *49*, 6260–6266; *Angew. Chem.* **2010**, *122*, 6400; e) P. Horcajada, R. Gref, T. Baati, P. K. Allan, G. Maurin, P. Couvreur, G. Férey, R. E. Morris, C. Serre, *Chem. Rev.* **2012**, *112*, 1232–1268.
[5] N. Stock, S. Biswas, *Chem. Rev.* **2012**, *112*, 933–969.
[6] a) Z. Wang, S. M. Cohen, *Chem. Soc. Rev.* **2009**, *38*, 1315–1329; b) K. K. Tanabe, S. M. Cohen, *Chem. Soc. Rev.* **2011**, *40*, 498–519; c) S. M. Cohen, *Chem. Sci.* **2010**, *1*, 32–36.
[7] a) M. Kim, J. F. Cahill, H. Fei, K. A. Prather, S. M. Cohen, *J. Am. Chem. Soc.* **2012**, *134*, 18082–18088; b) P. Deria, J. E. Mondloch, O. Karagiaridi, W. Bury, J. T. Hupp, O. K. Farha, *Chem. Soc. Rev.* **2014**, *43*, 5896–5912; c) C. K. Brozek, M. Dinca, *Chem. Soc. Rev.* **2014**, *43*, 5456–5467; d) J. D. Evans, C. J. Sumby, C. J. Doonan, *Chem. Soc. Rev.* **2014**, *43*, 5933–5951.
[8] Y. Bai, Y. Dou, L.-H. Xie, W. Rutledge, J.-R. Li, H.-C. Zhou, *Chem. Soc. Rev.* **2016**, *45*, 2327–2367.
[9] a) J. B. DeCoste, G. W. Peterson, H. Jasuja, T. G. Glover, Y.-G. Huang, K. S. Walton, *J. Mater. Chem. A* **2013**, *1*, 5642–5650; b) J. E. Mondloch, M. J. Katz, N. Planas, D. Semrouni, L. Gagliardi, J. T. Hupp, O. K. Farha, *Chem. Commun.* **2014**, *50*, 8944–8946; c) M. Kandiah, M. H. Nilsen, S. Usseglio, S. Jakobsen, U. Olsbye, M. Tilset, C. Larabi, E. A. Quadrelli, F. Bonino, K. P. Lillerud, *Chem. Mater.* **2010**, *22*, 6632–6640.
[10] a) H. Wu, T. Yildirim, W. Zhou, *J. Phys. Chem. Lett.* **2013**, *4*, 925–930; b) P. G. Yot, K. Yang, F. Ragon, V. Dmitriev, T. Devic, P. Horcajada, C. Serre, G. Maurin, *Dalton Trans.* **2016**, *45*, 4283–4288; c) R. J. Marshall, T. Richards, C. Hobday, C. F. Murphie, C. Wilson, S. A. Moggach, T. D. Bennett, R. S. Forgan, *Dalton Trans.* **2016**, *45*, 4132–4135; d) C. L. Hobday, R. J. Marshall, C. F. Murphie, J. Sotelo, T. Richards, D. R. Allan, T. Düren, F.-X. Coudert, R. S. Forgan, C. A. Morrison, S. A. Moggach, T. D. Bennett, *Angew. Chem. Int. Ed.* **2016**, *55*, 2401–2405; *Angew. Chem.* **2016**, *128*, 2447–2451; e) L.-M. Yang, E. Ganz, S. Svelle, M. Tilset, *J. Mater. Chem. C* **2014**, *2*, 7111–7125; f) B. Van de Voorde, I. Stassen, B. Bueken, F. Vermoortele, D. De Vos, R. Ameloot, J.-C. Tan, T. D. Bennett, *J. Mater. Chem. A* **2015**, *3*, 1737–1742.
[11] J. H. Cavka, S. Jakobsen, U. Olsbye, N. Guillou, C. Lamberti, S. Bordiga, K. P. Lillerud, *J. Am. Chem. Soc.* **2008**, *130*, 13850–13851.
[12] Z. Hu, D. Zhao, *Dalton Trans.* **2015**, *44*, 19018–19040.
[13] A. Schaate, P. Roy, T. Preuße, S. J. Lohmeier, A. Godt, P. Behrens, *Chem. Eur. J.* **2011**, *17*, 9320–9325.
[14] V. Guillerm, F. Ragon, M. Dan-Hardi, T. Devic, M. Vishnuvarthan, B. Campo, A. Vimont, G. Clet, Q. Yang, G. Maurin, G. Férey, A. Vittadini, S. Gross, C. Serre, *Angew. Chem. Int. Ed.* **2012**, *51*, 9267–9271; *Angew. Chem.* **2012**, *124*, 9401.

[15] J. Ma, A. G. Wong-Foy, A. J. Matzger, *Inorg. Chem.* **2015**, *54*, 4591–4593.
[16] a) R. Wang, Z. Wang, Y. Xu, F. Dai, L. Zhang, D. Sun, *Inorg. Chem.* **2014**, *53*, 7086–7088; b) H. Furukawa, F. Gándara, Y.-B. Zhang, J. Jiang, W. L. Queen, M. R. Hudson, O. M. Yaghi, *J. Am. Chem. Soc.* **2014**, *136*, 4369–4381; c) W. Liang, H. Chevreau, F. Ragon, P. D. Southon, V. K. Peterson, D. M. D'Alessandro, *CrystEngComm* **2014**, *16*, 6530–6533.
[17] a) D. Feng, Z.-Y. Gu, J.-R. Li, H.-L. Jiang, Z. Wei, H.-C. Zhou, *Angew. Chem. Int. Ed.* **2012**, *51*, 10307–10310; *Angew. Chem.* **2012**, *124*, 10453; b) W. Morris, B. Volosskiy, S. Demir, F. Gándara, P. L. McGrier, H. Furukawa, D. Cascio, J. F. Stoddart, O. M. Yaghi, *Inorg. Chem.* **2012**, *51*, 6443–6445.
[18] J. E. Mondloch, W. Bury, D. Fairen-Jimenez, S. Kwon, E. J. DeMarco, M. H. Weston, A. A. Sarjeant, S. T. Nguyen, P. C. Stair, R. Q. Snurr, O. K. Farha, J. T. Hupp, *J. Am. Chem. Soc.* **2013**, *135*, 10294–10297.
[19] D. Feng, H.-L. Jiang, Y.-P. Chen, Z.-Y. Gu, Z. Wei, H.-C. Zhou, *Inorg. Chem.* **2013**, *52*, 12661–12667.
[20] Q. Zhang, J. Su, D. Feng, Z. Wei, X. Zou, H.-C. Zhou, *J. Am. Chem. Soc.* **2015**, *137*, 10064–10067.
[21] G. Mouchaham, L. Cooper, N. Guillou, C. Martineau, E. Elkaïm, S. Bourrelly, P. L. Llewellyn, C. Allain, G. Clavier, C. Serre, T. Devic, *Angew. Chem. Int. Ed.* **2015**, *54*, 13297–13301; *Angew. Chem.* **2015**, *127*, 13495.
[22] a) C. G. Piscopo, A. Polyzoidis, M. Schwarzer, S. Loebbecke, *Microporous Mesoporous Mater.* **2015**, *208*, 30–35; b) H.-L. Jiang, D. Feng, K. Wang, Z.-Y. Gu, Z. Wei, Y.-P. Chen, H.-C. Zhou, *J. Am. Chem. Soc.* **2013**, *135*, 13934–13938.
[23] M. Kim, S. M. Cohen, *CrystEngComm* **2012**, *14*, 4096–4104.
[24] S. J. Garibay, S. M. Cohen, *Chem. Commun.* **2010**, *46*, 7700–7702.
[25] M. Servalli, M. Ranocchiari, J. A. Van Bokhoven, *Chem. Commun.* **2012**, *48*, 1904–1906.
[26] H. Hintz, S. Wuttke, *Chem. Mater.* **2014**, *26*, 6722–6728.
[27] W. Morris, C. J. Doonan, O. M. Yaghi, *Inorg. Chem.* **2011**, *50*, 6853–6855.
[28] Y. Luan, Y. Qi, H. Gao, R. S. Andriamitantsoa, N. Zheng, G. Wang, *J. Mater. Chem. A* **2015**, *3*, 17320–17331.
[29] J. Bonnefoy, A. Legrand, E. A. Quadrelli, J. Canivet, D. Farrusseng, *J. Am. Chem. Soc.* **2015**, *137*, 9409–9416.
[30] Y. Zhang, X. Feng, H. Li, Y. Chen, J. Zhao, S. Wang, L. Wang, B. Wang, *Angew. Chem. Int. Ed.* **2015**, *54*, 4259–4263; *Angew. Chem.* **2015**, *127*, 4333.
[31] M. Kim, S. J. Garibay, S. M. Cohen, *Inorg. Chem.* **2011**, *50*, 729–731.
[32] P. Roy, A. Schaate, P. Behrens, A. Godt, *Chem. Eur. J.* **2012**, *18*, 6979–6985.
[33] B. Li, B. Gui, G. Hu, D. Yuan, C. Wang, *Inorg. Chem.* **2015**, *54*, 5139–5141.
[34] H.-L. Jiang, D. Feng, T.-F. Liu, J.-R. Li, H.-C. Zhou, *J. Am. Chem. Soc.* **2012**, *134*, 14690–14693.
[35] T. Ishiwata, Y. Furukawa, K. Sugikawa, K. Kokado, K. Sada, *J. Am. Chem. Soc.* **2013**, *135*, 5427–5432.
[36] X.-C. Yi, F.-G. Xi, Y. Qi, E.-Q. Gao, *RSC Adv.* **2015**, *5*, 893–900.
[37] B. Gui, G. Hu, T. Zhou, C. Wang, *J. Solid State Chem.* **2015**, *223*, 79–83.
[38] K. Hindelang, A. Kronast, S. I. Vagin, B. Rieger, *Chem. Eur. J.* **2013**, *19*, 8244–8252.
[39] a) Q. Yang, A. D. Wiersum, P. L. Llewellyn, V. Guillerm, C. Serre, G. Maurin, *Chem. Commun.* **2011**, *47*, 9603–9605; b) A. Torrisi, C. Mellot-Draznieks, R. G. Bell, *J. Chem. Phys.* **2010**, *132*, 044705.
[40] A. Shigematsu, T. Yamada, H. Kitagawa, *J. Am. Chem. Soc.* **2011**, *133*, 2034–2036.
[41] W. J. Phang, H. Jo, W. R. Lee, J. H. Song, K. Yoo, B. Kim, C. S. Hong, *Angew. Chem. Int. Ed.* **2015**, *54*, 5142–5146; *Angew. Chem.* **2015**, *127*, 5231.
[42] F. Ragon, B. Campo, Q. Yang, C. Martineau, A. D. Wiersum, A. Lago, V. Guillerm, C. Hemsley, J. F. Eubank, M. Vishnuvarthan, F. Taulelle, P. Horcajada, A. Vimont, P. L. Llewellyn, M. Daturi, S. Devautour-Vinot, G. Maurin, C. Serre, T. Devic, G. Clet, *J. Mater. Chem. A* **2015**, *3*, 3294–3309.
[43] B. Gui, X. Meng, Y. Chen, J. Tian, G. Liu, C. Shen, M. Zeller, D. Yuan, C. Wang, *Chem. Mater.* **2015**, *27*, 6426–6431.
[44] J. Aguilera-Sigalat, A. Fox-Charles, D. Bradshaw, *Chem. Commun.* **2014**, *50*, 15453–15456.
[45] J. B. DeCoste, M. A. Browe, G. W. Wagner, J. A. Rossin, G. W. Peterson, *Chem. Commun.* **2015**, *51*, 12474–12477.
[46] Q. Zhang, J. Yu, J. Cai, L. Zhang, Y. Cui, Y. Yang, B. Chen, G. Qian, *Chem. Commun.* **2015**, *51*, 14732–14734.
[47] R. J. Marshall, S. L. Griffin, C. Wilson, R. S. Forgan, *J. Am. Chem. Soc.* **2015**, *137*, 9527–9530.
[48] R. J. Marshall, S. L. Griffin, C. Wilson, R. S. Forgan, *Chem. Eur. J.* **2016**, *22*, 4870–4877.
[49] C. V. McGuire, R. S. Forgan, *Chem. Commun.* **2015**, *51*, 5199–5217.
[50] J. Chun, S. Kang, N. Park, E. J. Park, X. Jin, K.-D. Kim, H. O. Seo, S. M. Lee, H. J. Kim, W. H. Kwon, Y.-K. Park, J. M. Kim, Y. D. Kim, S. U. Son, *J. Am. Chem. Soc.* **2014**, *136*, 6786–6789.
[51] S. Nagata, K. Kokado, K. Sada, *Chem. Commun.* **2015**, *51*, 8614–8617.
[52] S. R. Venna, M. Lartey, T. Li, A. Spore, S. Kumar, H. B. Nulwala, D. R. Luebke, N. L. Rosi, E. Albenze, *J. Mater. Chem. A* **2015**, *3*, 5014–5022.
[53] C. He, K. Lu, D. Liu, W. Lin, *J. Am. Chem. Soc.* **2014**, *136*, 5181–5184.
[54] S. Wang, W. Morris, Y. Liu, C. M. McGuirk, Y. Zhou, J. T. Hupp, O. K. Farha, C. A. Mirkin, *Angew. Chem. Int. Ed.* **2015**, *54*, 14738–14742; *Angew. Chem.* **2015**, *127*, 14951.
[55] W. Morris, W. E. Briley, E. Auyeung, M. D. Cabezas, C. A. Mirkin, *J. Am. Chem. Soc.* **2014**, *136*, 7261–7264.
[56] S. Chavan, J. G. Vitillo, M. J. Uddin, F. Bonino, C. Lamberti, E. Groppo, K.-P. Lillerud, S. Bordiga, *Chem. Mater.* **2010**, *22*, 4602–4611.
[57] a) M. Lin Foo, S. Horike, T. Fukushima, Y. Hijikata, Y. Kubota, M. Takata, S. Kitagawa, *Dalton Trans.* **2012**, *41*, 13791–13794; b) Z. Hu, K. Zhang, M. Zhang, Z. Guo, J. Jiang, D. Zhao, *ChemSusChem* **2014**, *7*, 2791–2795.
[58] Z. Hu, M. Khurana, Y. H. Seah, M. Zhang, Z. Guo, D. Zhao, *Chem. Eng. Sci.* **2015**, *124*, 61–69.
[59] L. Li, S. Tang, C. Wang, X. Lv, M. Jiang, H. Wu, X. Zhao, *Chem. Commun.* **2014**, *50*, 2304–2307.
[60] M. I. Gonzalez, E. D. Bloch, J. A. Mason, S. J. Teat, J. R. Long, *Inorg. Chem.* **2015**, *54*, 2995–3005.
[61] K. Manna, T. Zhang, W. Lin, *J. Am. Chem. Soc.* **2014**, *136*, 6566–6569.
[62] X. Yu, S. M. Cohen, *Chem. Commun.* **2015**, *51*, 9880–9883.
[63] H. Fei, M. D. Sampson, Y. Lee, C. P. Kubiak, S. M. Cohen, *Inorg. Chem.* **2015**, *54*, 6821–6828.
[64] X. Lin, Y. Hong, C. Zhang, R. Huang, C. Wang, W. Lin, *Chem. Commun.* **2015**, *51*, 16996–16999.
[65] Y. Zhou, B. Yan, *Chem. Commun.* **2016**, *52*, 2265–2268.
[66] H. Fei, J. Shin, Y. S. Meng, M. Adelhardt, J. Sutter, K. Meyer, S. M. Cohen, *J. Am. Chem. Soc.* **2014**, *136*, 4965–4973.
[67] Y. Lee, S. Kim, H. Fei, J. K. Kang, S. M. Cohen, *Chem. Commun.* **2015**, *51*, 16549–16552.
[68] H. Fei, S. M. Cohen, *J. Am. Chem. Soc.* **2015**, *137*, 2191–2194.
[69] K. Manna, T. Zhang, M. Carboni, C. W. Abney, W. Lin, *J. Am. Chem. Soc.* **2014**, *136*, 13182–13185.
[70] K. Manna, T. Zhang, F. X. Greene, W. Lin, *J. Am. Chem. Soc.* **2015**, *137*, 2665–2673.
[71] J. M. Falkowski, T. Sawano, T. Zhang, G. Tsun, Y. Chen, J. V. Lockard, W. Lin, *J. Am. Chem. Soc.* **2014**, *136*, 5213–5216.
[72] T. Sawano, N. C. Thacker, Z. Lin, A. R. McIsaac, W. Lin, *J. Am. Chem. Soc.* **2015**, *137*, 12241–12248.
[73] T. Sawano, P. Ji, A. R. McIsaac, Z. Lin, C. W. Abney, W. Lin, *Chem. Sci.* **2015**, *6*, 7163–7168.
[74] C.-W. Kung, T.-H. Chang, L.-Y. Chou, J. T. Hupp, O. K. Farha, K.-C. Ho, *Chem. Commun.* **2015**, *51*, 2414–2417.
[75] J. Zheng, M. Wu, F. Jiang, W. Su, M. Hong, *Chem. Sci.* **2015**, *6*, 3466–3470.
[76] O. Karagiaridi, W. Bury, J. E. Mondloch, J. T. Hupp, O. K. Farha, *Angew. Chem. Int. Ed.* **2014**, *53*, 4530–4540; *Angew. Chem.* **2014**, *126*, 4618.
[77] M. Kim, J. F. Cahill, Y. Su, K. A. Prather, S. M. Cohen, *Chem. Sci.* **2012**, *3*, 126–130.
[78] S. Pullen, H. Fei, A. Orthaber, S. M. Cohen, S. Ott, *J. Am. Chem. Soc.* **2013**, *135*, 16997–17003.
[79] H. Fei, S. Pullen, A. Wagner, S. Ott, S. M. Cohen, *Chem. Commun.* **2015**, *51*, 66–69.
[80] Z. Hu, S. Faucher, Y. Zhuo, Y. Sun, S. Wang, D. Zhao, *Chem. Eur. J.* **2015**, *21*, 17246–17255.
[81] D. H. Hong, M. P. Suh, *Chem. Eur. J.* **2014**, *20*, 426–434.
[82] F. Carson, E. Martinez-Castro, R. Marcos, G. G. Miera, K. Jansson, X. Zou, B. Martin-Matute, *Chem. Commun.* **2015**, *51*, 10864–10867.
[83] a) K. E. deKrafft, W. S. Boyle, L. M. Burk, O. Z. Zhou, W. Lin, *J. Mater. Chem.* **2012**, *22*, 18139–18144; b) S. Jakobsen, D. Gianolio, D. S. Wragg, M. H. Nilsen, H. Emerich, S. Bordiga, C. Lamberti, U. Olsbye, M. Tilset, K. P. Lillerud, *Phys. Rev. B* **2012**, *86*, 125429.
[84] C. Falaise, C. Volkringer, J.-F. Vigier, N. Henry, A. Beaurain, T. Loiseau, *Chem. Eur. J.* **2013**, *19*, 5324–5331.

[85] C. Falaise, J.-S. Charles, C. Volkringer, T. Loiseau, *Inorg. Chem.* **2015**, *54*, 2235–2242.
[86] M. Lammert, M. T. Wharmby, S. Smolders, B. Bueken, A. Lieb, K. A. Lomachenko, D. De Vos, N. Stock, *Chem. Commun.* **2015**, *51*, 12578–12581.
[87] H. G. T. Nguyen, L. Mao, A. W. Peters, C. O. Audu, Z. J. Brown, O. K. Farha, J. T. Hupp, S. T. Nguyen, *Catal. Sci. Technol.* **2015**, *5*, 4444–4451.
[88] C. Hon Lau, R. Babarao, M. R. Hill, *Chem. Commun.* **2013**, *49*, 3634–3636.
[89] S. J. D. Smith, B. P. Ladewig, A. J. Hill, C. H. Lau, M. R. Hill, *Sci. Rep.* **2015**, *5*, 7823.
[90] D. Sun, W. Liu, M. Qiu, Y. Zhang, Z. Li, *Chem. Commun.* **2015**, *51*, 2056–2059.
[91] Y. Lee, S. Kim, J. K. Kang, S. M. Cohen, *Chem. Commun.* **2015**, *51*, 5735–5738.
[92] a) G. Wißmann, A. Schaate, S. Lilienthal, I. Bremer, A. M. Schneider, P. Behrens, *Microporous Mesoporous Mater.* **2012**, *152*, 64–70; b) A. Schaate, S. Dühnen, G. Platz, S. Lilienthal, A. M. Schneider, P. Behrens, *Eur. J. Inorg. Chem.* **2012**, 790–796.
[93] G. Zahn, P. Zerner, J. Lippke, F. L. Kempf, S. Lilienthal, C. A. Schroder, A. M. Schneider, P. Behrens, *CrystEngComm* **2014**, *16*, 9198–9207.
[94] V. Guillerm, S. Gross, C. Serre, T. Devic, M. Bauer, G. Férey, *Chem. Commun.* **2010**, *46*, 767–769.
[95] a) O. V. Gutov, M. G. Hevia, E. C. Escudero-Adán, A. Shafir, *Inorg. Chem.* **2015**, *54*, 8396–8400; b) M. J. Katz, Z. J. Brown, Y. J. Colon, P. W. Siu, K. A. Scheidt, R. Q. Snurr, J. T. Hupp, O. K. Farha, *Chem. Commun.* **2013**, *49*, 9449–9451; c) G. C. Shearer, S. Chavan, J. Ethiraj, J. G. Vitillo, S. Svelle, U. Olsbye, C. Lamberti, S. Bordiga, K. P. Lillerud, *Chem. Mater.* **2014**, *26*, 4068–4071; d) H. Wu, Y. S. Chua, V. Krungleviciute, M. Tyagi, P. Chen, T. Yildirim, W. Zhou, *J. Am. Chem. Soc.* **2013**, *135*, 10525–10532; e) Z. Fang, B. Bueken, D. E. De Vos, R. A. Fischer, *Angew. Chem. Int. Ed.* **2015**, *54*, 7234–7254; *Angew. Chem.* **2015**, *127*, 7340.
[96] C. A. Trickett, K. J. Gagnon, S. Lee, F. Gándara, H.-B. Bürgi, O. M. Yaghi, *Angew. Chem. Int. Ed.* **2015**, *54*, 11162–11167; *Angew. Chem.* **2015**, *127*, 11314.
[97] Y. Han, M. Liu, K. Li, Y. Zuo, Y. Wei, S. Xu, G. Zhang, C. Song, Z. Zhang, X. Guo, *CrystEngComm* **2015**, *17*, 6434–6440.
[98] F. Vermoortele, B. Bueken, G. Le Bars, B. Van de Voorde, M. Vandichel, K. Houthoofd, A. Vimont, M. Daturi, M. Waroquier, V. Van Speybroeck, C. Kirschhock, D. E. De Vos, *J. Am. Chem. Soc.* **2013**, *135*, 11465–11468.
[99] R. J. Marshall, C. L. Hobday, C. F. Murphie, S. L. Griffin, C. A. Morrison, S. A. Moggach, R. S. Forgan, *J. Mater. Chem. A* **2016**, *4*, 6955–6963.
[100] J. M. Taylor, S. Dekura, R. Ikeda, H. Kitagawa, *Chem. Mater.* **2015**, *27*, 2286–2289.
[101] S. Yuan, W. Lu, Y.-P. Chen, Q. Zhang, T.-F. Liu, D. Feng, X. Wang, J. Qin, H.-C. Zhou, *J. Am. Chem. Soc.* **2015**, *137*, 3177–3180.
[102] R. C. Klet, Y. Liu, T. C. Wang, J. T. Hupp, O. K. Farha, *J. Mater. Chem. A* **2016**, *4*, 1479–1485.
[103] J. B. DeCoste, T. J. Demasky, M. J. Katz, O. K. Farha, J. T. Hupp, *New J. Chem.* **2015**, *39*, 2396–2399.
[104] L.-J. Li, P.-Q. Liao, C.-T. He, Y.-S. Wei, H.-L. Zhou, J.-M. Lin, X.-Y. Li, J.-P. Zhang, *J. Mater. Chem. A* **2015**, *3*, 21849–21855.
[105] P. Deria, J. E. Mondloch, E. Tylianakis, P. Ghosh, W. Bury, R. Q. Snurr, J. T. Hupp, O. K. Farha, *J. Am. Chem. Soc.* **2013**, *135*, 16801–16804.
[106] P. Deria, Y. G. Chung, R. Q. Snurr, J. T. Hupp, O. K. Farha, *Chem. Sci.* **2015**, *6*, 5172–5176.
[107] Y.-B. Huang, M. Shen, X. Wang, P. Huang, R. Chen, Z.-J. Lin, R. Cao, *J. Catal.* **2016**, *333*, 1–7.
[108] P. Deria, S. Li, H. Zhang, R. Q. Snurr, J. T. Hupp, O. K. Farha, *Chem. Commun.* **2015**, *51*, 12478–12481.
[109] P. Deria, W. Bury, J. T. Hupp, O. K. Farha, *Chem. Commun.* **2014**, *50*, 1965–1968.
[110] I. Hod, W. Bury, D. M. Gardner, P. Deria, V. Roznyatovskiy, M. R. Wasielewski, O. K. Farha, J. T. Hupp, *J. Phys. Chem. Lett.* **2015**, *6*, 586–591.
[111] P. R. McGonigal, P. Deria, I. Hod, P. Z. Moghadam, A.-J. Avestro, N. E. Horwitz, I. C. Gibbs-Hall, A. K. Blackburn, D. Chen, Y. Y. Botros, M. R. Wasielewski, R. Q. Snurr, J. T. Hupp, O. K. Farha, J. F. Stoddart, *Proc. Natl. Acad. Sci. USA* **2015**, *112*, 11161–11168.
[112] S.-Y. Moon, A. J. Howarth, T. Wang, N. A. Vermeulen, J. T. Hupp, O. K. Farha, *Chem. Commun.* **2016**, *52*, 3438–3441.
[113] P. Deria, W. Bury, I. Hod, C.-W. Kung, O. Karagiaridi, J. T. Hupp, O. K. Farha, *Inorg. Chem.* **2015**, *54*, 2185–2192.
[114] a) M. J. Katz, J. E. Mondloch, R. K. Totten, J. K. Park, S. T. Nguyen, O. K. Farha, J. T. Hupp, *Angew. Chem. Int. Ed.* **2014**, *53*, 497–501; *Angew. Chem.* **2014**, *126*, 507; b) M. J. Katz, S.-Y. Moon, J. E. Mondloch, M. H. Beyzavi, C. J. Stephenson, J. T. Hupp, O. K. Farha, *Chem. Sci.* **2015**, *6*, 2286–2291.
[115] a) J. E. Mondloch, M. J. Katz, W. C. Isley III, P. Ghosh, P. Liao, W. Bury, G. W. Wagner, M. G. Hall, J. B. DeCoste, G. W. Peterson, R. Q. Snurr, C. J. Cramer, J. T. Hupp, O. K. Farha, *Nat. Mater.* **2015**, *14*, 512–516; b) S.-Y. Moon, Y. Liu, J. T. Hupp, O. K. Farha, *Angew. Chem. Int. Ed.* **2015**, *54*, 6795–6799; *Angew. Chem.* **2015**, *127*, 6899.
[116] S. T. Madrahimov, J. R. Gallagher, G. Zhang, Z. Meinhart, S. J. Garibay, M. Delferro, J. T. Miller, O. K. Farha, J. T. Hupp, S. T. Nguyen, *ACS Catal.* **2015**, *5*, 6713–6718.
[117] I. L. Malaestean, M. Speldrich, A. Ellern, S. G. Baca, P. Kogerler, *Dalton Trans.* **2011**, *40*, 331–333.
[118] C. Larabi, E. A. Quadrelli, *Eur. J. Inorg. Chem.* **2012**, 3014–3022.
[119] R. Ameloot, M. Aubrey, B. M. Wiers, A. P. Gómora-Figueroa, S. N. Patel, N. P. Balsara, J. R. Long, *Chem. Eur. J.* **2013**, *19*, 5533–5536.
[120] E. López-Maya, C. Montoro, L. M. Rodríguez-Albelo, S. D. Aznar Cervantes, A. A. Lozano-Pérez, J. L. Cenís, E. Barea, J. A. R. Navarro, *Angew. Chem. Int. Ed.* **2015**, *54*, 6790–6794; *Angew. Chem.* **2015**, *127*, 6894.
[121] H. G. T. Nguyen, N. M. Schweitzer, C.-Y. Chang, T. L. Drake, M. C. So, P. C. Stair, O. K. Farha, J. T. Hupp, S. T. Nguyen, *ACS Catal.* **2014**, *4*, 2496–2500.
[122] a) D. Yang, S. O. Odoh, T. C. Wang, O. K. Farha, J. T. Hupp, C. J. Cramer, L. Gagliardi, B. C. Gates, *J. Am. Chem. Soc.* **2015**, *137*, 7391–7396; b) D. Yang, S. O. Odoh, J. Borycz, T. C. Wang, O. K. Farha, J. T. Hupp, C. J. Cramer, L. Gagliardi, B. C. Gates, *ACS Catal.* **2016**, *6*, 235–247.
[123] S. Yuan, Y.-P. Chen, J. Qin, W. Lu, X. Wang, Q. Zhang, M. Bosch, T.-F. Liu, X. Lian, H.-C. Zhou, *Angew. Chem. Int. Ed.* **2015**, *54*, 14696–14700; *Angew. Chem.* **2015**, *127*, 14909.
[124] R. C. Klet, T. C. Wang, L. E. Fernandez, D. G. Truhlar, J. T. Hupp, O. K. Farha, *Chem. Mater.* **2016**, *28*, 1213–1219.
[125] C.-W. Kung, J. E. Mondloch, T. C. Wang, W. Bury, W. Hoffeditz, B. M. Klahr, R. C. Klet, M. J. Pellin, O. K. Farha, J. T. Hupp, *ACS Appl. Mater. Interfaces* **2015**, *7*, 28223–28230.
[126] I. S. Kim, J. Borycz, A. E. Platero-Prats, S. Tussupbayev, T. C. Wang, O. K. Farha, J. T. Hupp, L. Gagliardi, K. W. Chapman, C. J. Cramer, A. B. F. Martinson, *Chem. Mater.* **2015**, *27*, 4772–4778.
[127] A. W. Peters, Z. Li, O. K. Farha, J. T. Hupp, *ACS Nano* **2015**, *9*, 8484–8490.
[128] Z. Li, N. M. Schweitzer, A. B. League, V. Bernales, A. W. Peters, A. B. Getsoian, T. C. Wang, J. T. Miller, A. Vjunov, J. L. Fulton, J. A. Lercher, C. J. Cramer, L. Gagliardi, J. T. Hupp, O. K. Farha, *J. Am. Chem. Soc.* **2016**, *138*, 1977–1982.

Received: April 5, 2016
Published Online: July 27, 2016